On Jet Noise Using Numerical Methods

W. Schröder, H. Foysi, G. Geiser, S. Koh

Institute of Aerodynamics, RWTH Aachen University
Wüllnerstr. 5a, 52062 Aachen, Germany

Coming Up

Introduction

Numerical Method

- flow field
- acoustic field

Results (Fluid Mechanics, Acoustics)

- single jet
  - → s (density ratio jet/freestream) = 1
  - → s > 1
  - → s < 1
- coaxial jet

Conclusions

Introduction

Jet aeroacoustics from aircraft engine exhaust is of great concern for

- communities near airports
- passengers
- structural integrity of the airframe

More industrial high pressure gas jets generating noise occur in

- valves
- burners
- miniature jets used for drying
- high pressure expansions in the power industry

Understanding the noise sources is a must to develop future passive and/or active noise reduction technologies

Coming Up

Introduction

Numerical Method

- flow field
- acoustic field

Results (Fluid Mechanics, Acoustics)

- single jet
  - $\rightarrow$ s (density ratio jet/freestream) = 1
  - $\rightarrow$ s > 1
  - $\rightarrow$ s < 1
- coaxial jet

Conclusions

Numerical Method

Two-Step Approach

1st step: flow analysis → large-eddy simulation

- tailored numerics for fluid flow
- focus on source region

2nd step: acoustics analysis → solution of acoustic equations

- tailored numerics for sound propagation
- extension from the source region to near far-field region

LES: Non-Reactive Multi-Species Flows

RWTH Aachen

compressible Navier-Stokes equations
for non-reactive multi-species flows

$$\frac{\partial \mathbf{Q}}{\partial \boldsymbol{t}} + \nabla \bullet (\mathbf{F}^{\mathrm{c}} - \mathbf{F}^{\mathrm{d}}) = 0 \qquad \mathbf{Q} = (\rho_n,\ \rho,\ \rho\mathbf{u}, \rho E_t)^{\mathrm{T}}$$

Euler flux

$$\mathbf{F}^{\mathrm{c}} = \begin{pmatrix} \rho_n \mathbf{u} \\ \rho \mathbf{u} \\ \rho \mathbf{u}\mathbf{u} + p\mathbf{I} \\ \mathbf{u}(\rho E_t + p) \end{pmatrix}$$

Non-Euler flux

$$\mathbf{F}^{\mathrm{d}} = \frac{1}{\mathrm{Re}} \begin{pmatrix} \mathbf{j}_n \\ 0 \\ \boldsymbol{\phi} \\ \boldsymbol{\phi} \cdot \mathbf{u} - \mathbf{q}_\beta - \sum h_n (\mathbf{j}_n)_\beta \end{pmatrix}$$

mass diffusion by Fick's law	equation of state for mixture of ideal gas	transport coefficients (function of temperature)
$\mathbf{j}_n = \frac{\rho D_n}{\mathrm{Sc}_0(\gamma_0)} Y_{,\beta}$	$p = \sum_n p_n$ with $p_n = \frac{T}{\gamma_0} \rho_n R_n$	$\ln \kappa_n^* = \sum_{i=1}^{5} (a_i^*)_n \ln(T^*)^{i-1}$

APE: Acoustic Perturbation Equations I

Basic ideas to derive the acoustic perturbation equations

1. Linearized Euler Equations (LEE) contain entropy, vorticity, and acoustic modes
2. APE focuses on acoustic modes
3. LEE to APE via source filtering, i.e.,

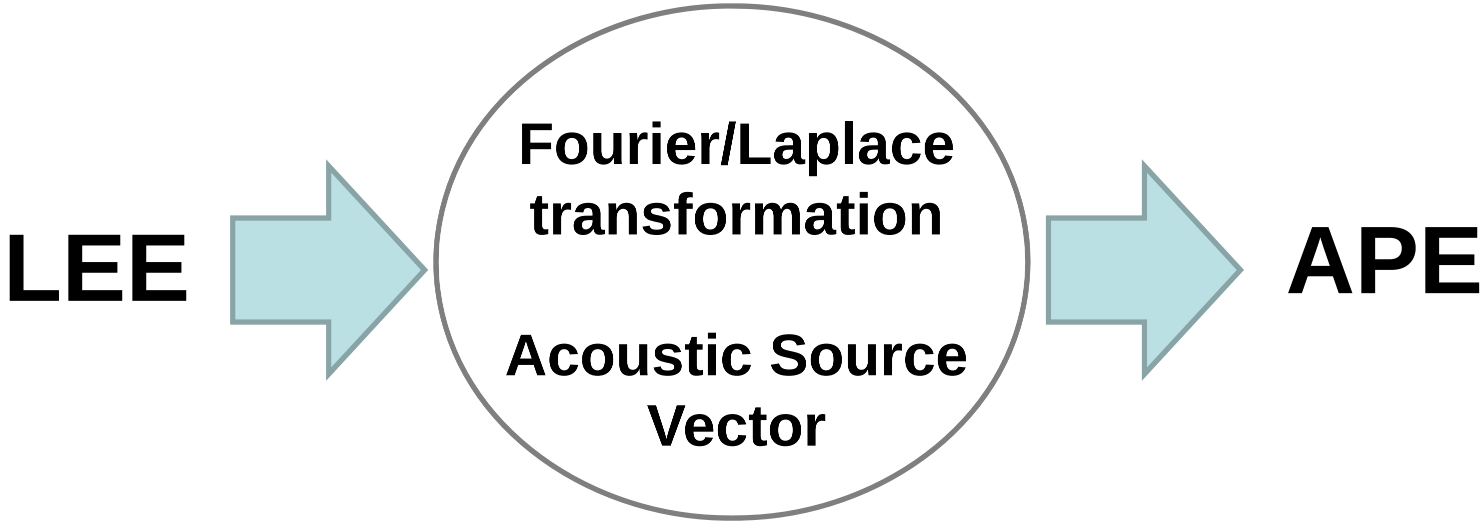

APE: Acoustic Perturbation Equations II

RWTH Aachen

- Ewert and Schröder, *J. Comput. Phys.*, 188, 2003.

APE-4 system

$$\frac{\partial p'}{\partial t} + \bar{a}^2 \nabla \cdot \left(\bar{\rho}\mathbf{u}' + \bar{\mathbf{u}}\frac{p'}{\bar{a}^2} \right) = \bar{a}^2 q_c$$

$$\frac{\partial \mathbf{u}'}{\partial t} + \nabla \left(\bar{\mathbf{u}} \cdot \mathbf{u}' \right) + \nabla \left(\frac{p'}{\bar{\rho}} \right) = \mathbf{q}_m \ ,$$

<u>objective</u>: easy to calculate the source terms in compressible flow governing equations

Source Terms

$$q_c = \boxed{-\nabla \cdot (\rho' \mathbf{u}')'} + \boxed{\frac{\bar{\rho}}{c_p}\frac{\bar{D}s'}{Dt}}$$

$$\mathbf{q}_m = \boxed{-(\boldsymbol{\omega} \times \mathbf{u})'} + \boxed{T'\nabla\bar{s} - s'\nabla\bar{T}} \boxed{- \left(\nabla \frac{(u')^2}{2} \right)'}$$

$\mathbf{L}'$: Lamb vector fluctuations

$\mathbf{Q}_e$: Entropy terms (linear approx.)

$\mathbf{Q}_n$: Nonlinear terms

Coming Up

Introduction

Numerical Method

- flow field
- acoustic field

Results (Fluid Mechanics, Acoustics)

- single jet
  - $\rightarrow$ s (density ratio jet/freestream) = 1
  - $\rightarrow$ s > 1
  - $\rightarrow$ s < 1
- coaxial jet

Conclusions

Isothermal Single Jet (ISJ)

Single Jet

- $Re_D = \rho_j U_j D/\mu_j = 400{,}000$
- $M_j = U_j/a_j = 0.9$
- Isothermal jet : $T_j = T_{ambient}$

- Generalized Coordinates
- 64-blocks (20,142,144 cells)
- $\Delta r_{MIN} = 0.02R$, $\Delta z = 0.07R$

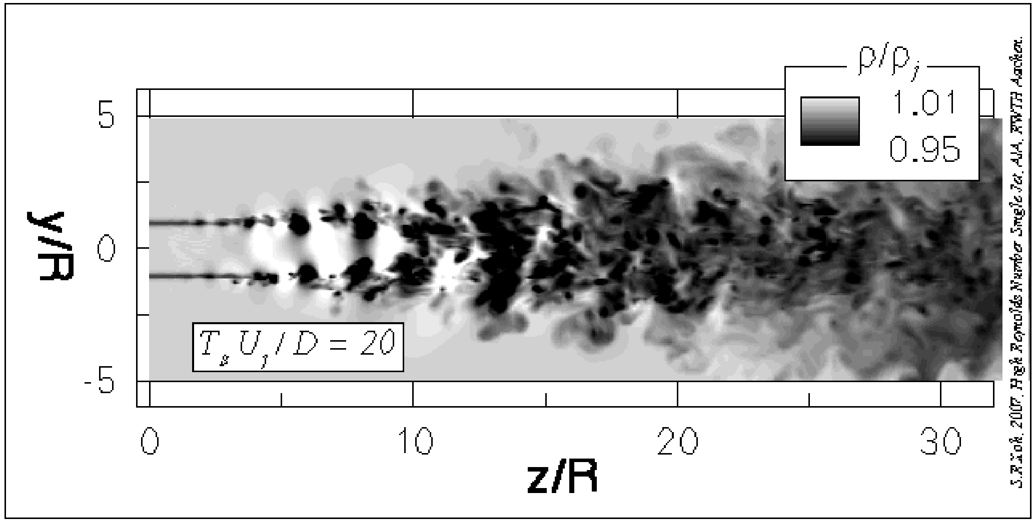

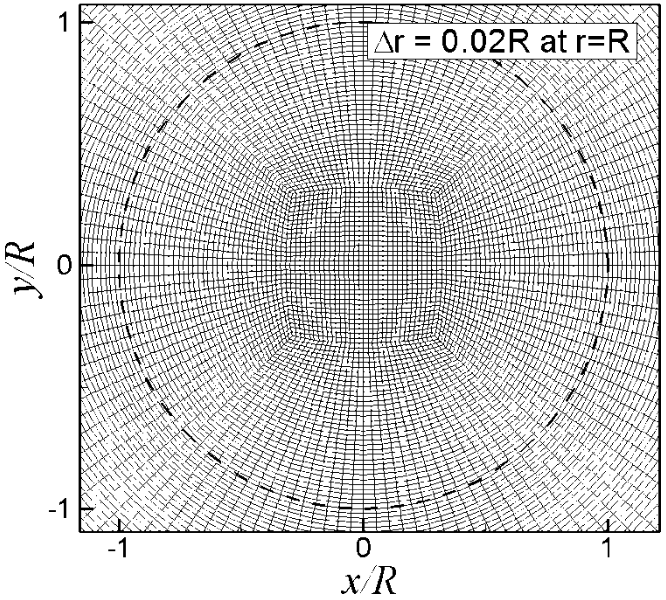

ISJ: Acoustic Field I

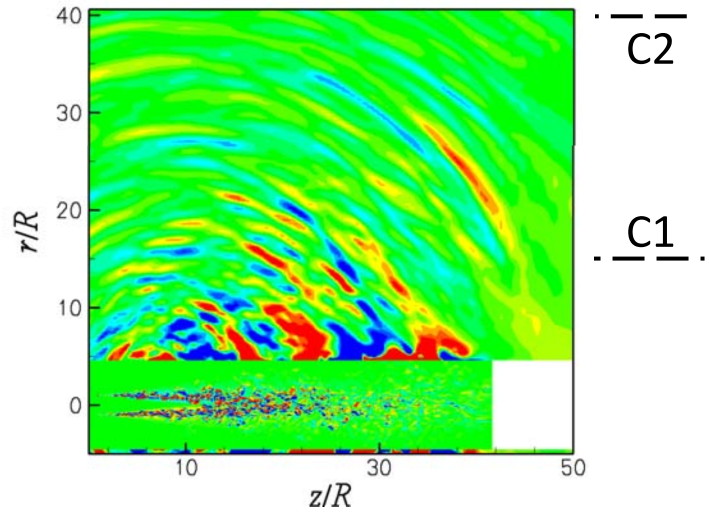

Instantaneous acoustic field

: Acoustic pressure and Lamb vector

LES_{BA}, EXP_{BA} : Barré et al. (2006)

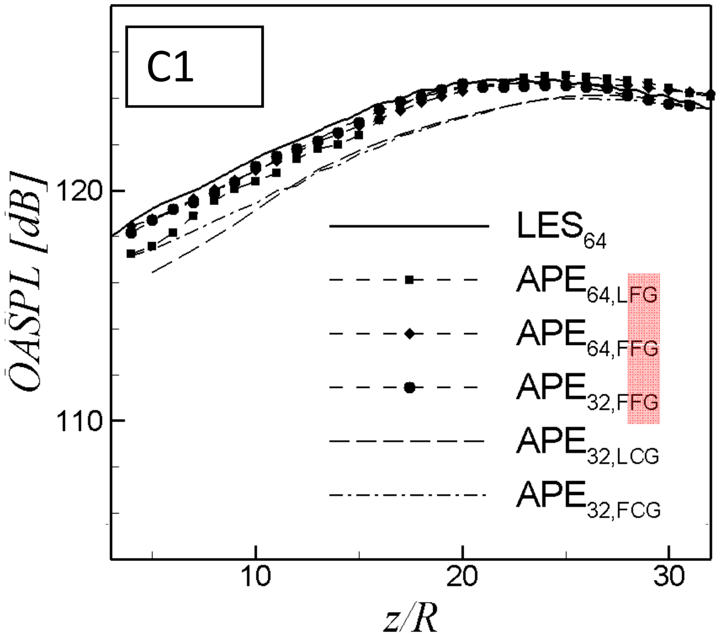

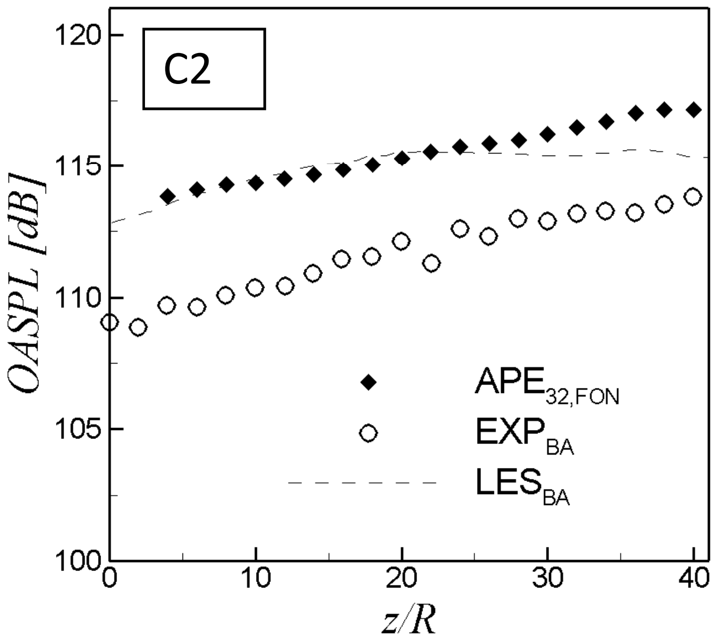

ISJ: Acoustic Field II

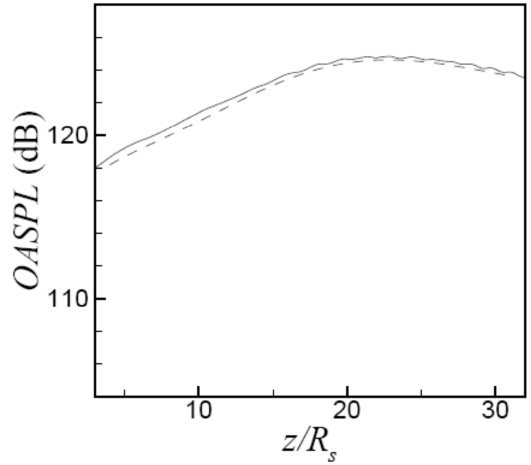

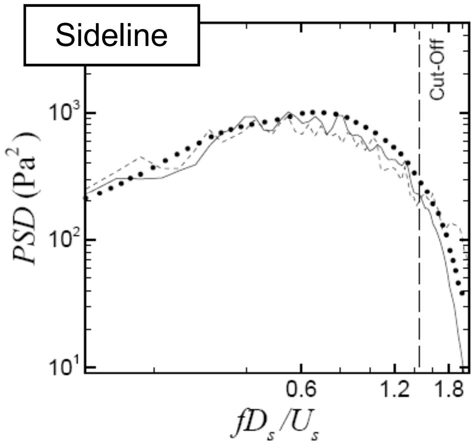

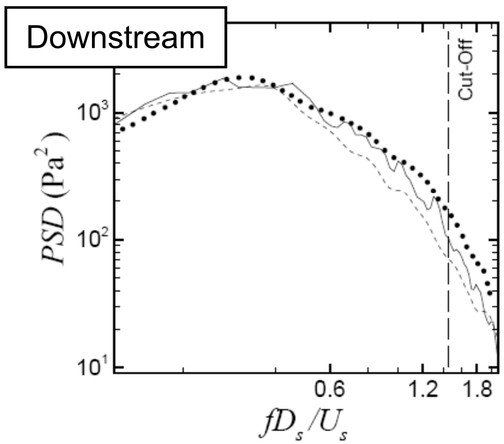

LES/APE
LES
Bogey&Bailly

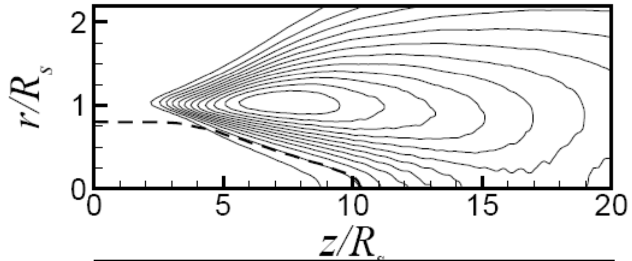

Turbulent Kinetic Energy

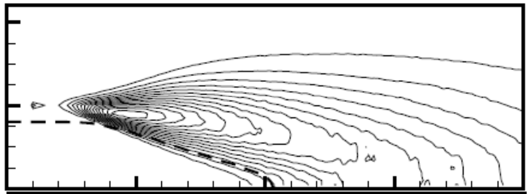

Lamb vector (rms)

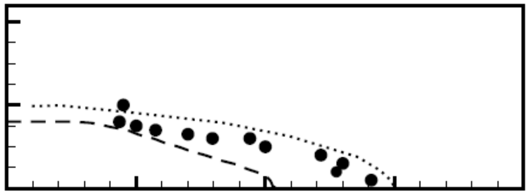

Lamb vector (Spectral peak)

Potential Core
Lamb vector Maxima

Coming Up

Introduction

Numerical Method

- flow field
- acoustic field

Results (Fluid Mechanics, Acoustics)

- single jet
  - $\rightarrow$ s (density ratio jet/freestream) = 1
  - $\rightarrow$ s > 1
  - $\rightarrow$ s < 1
- coaxial jet

Conclusions

Single Jet (SJ): $s = \rho_{jet} / \rho_{freestream} > 1$

RWTH Aachen

2 high-density jets are considered

- **CO_2 jet: $s \approx 1.5$**
- **cooled-air jet: $s \approx 1.5$**

SJ (s > 1): CO_2 Jet LES I

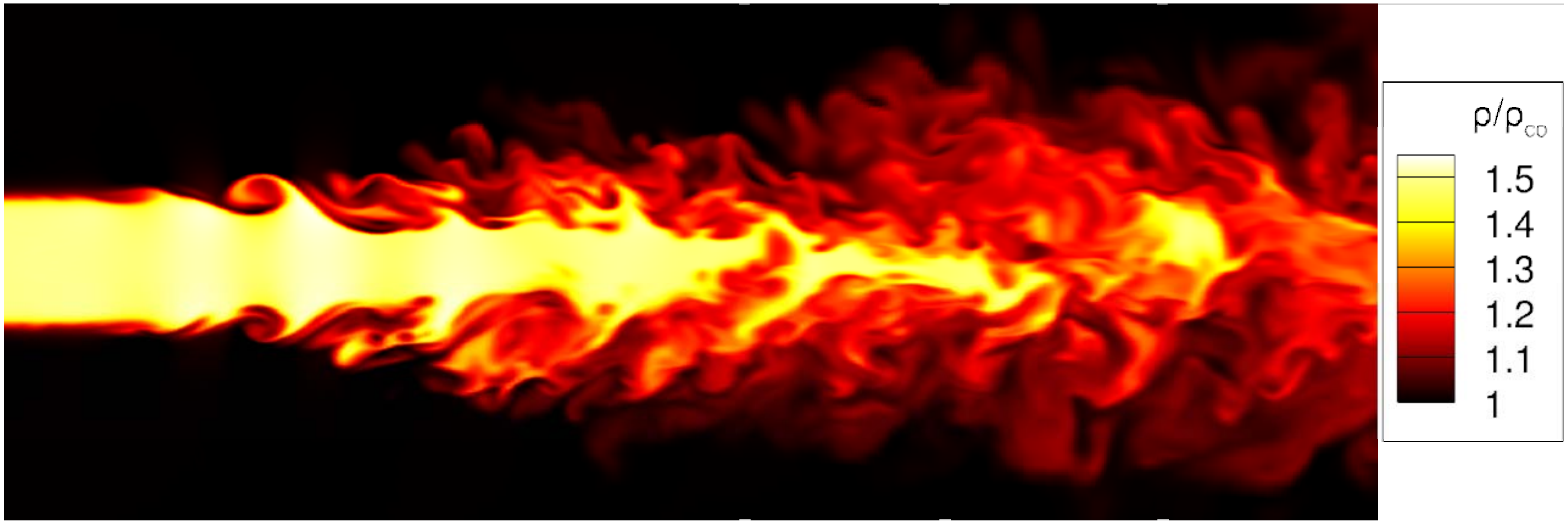

Mach number and Reynolds number based on centerline velocity and diameter: Ma = 0.6, Re_D = 26,666

SJ (s > 1): CO_2 Jet LES II

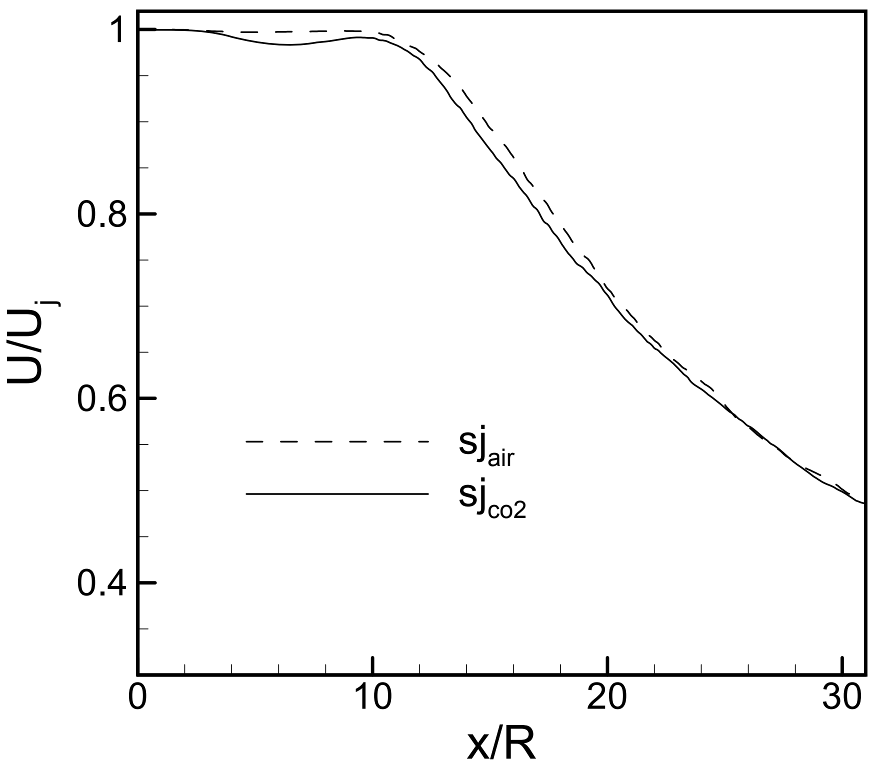

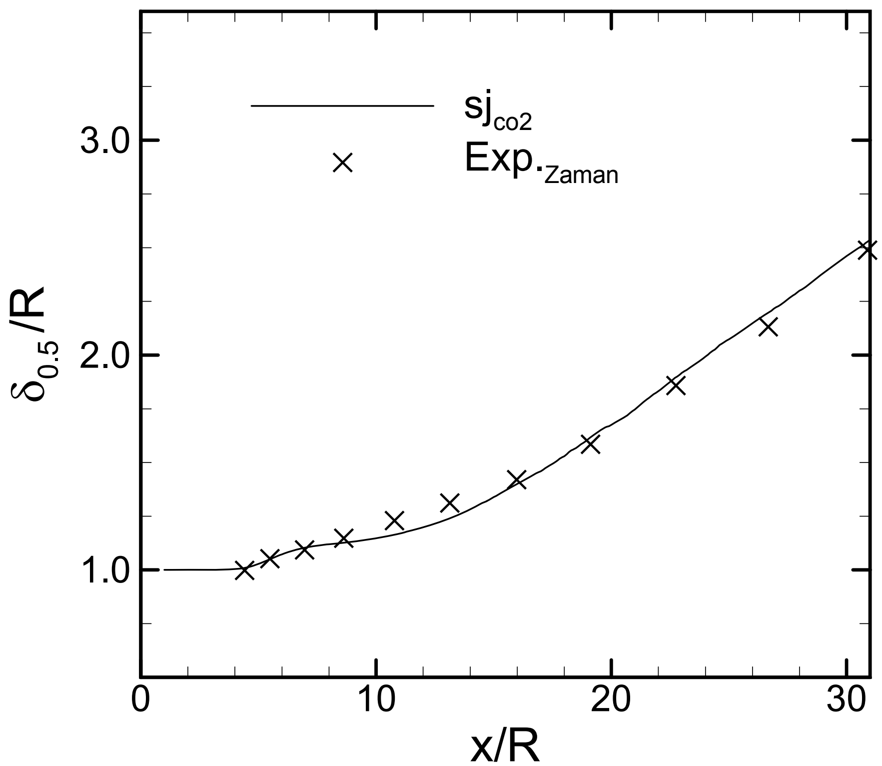

- **Centerline velocity decay matches the distribution of a pure air jet at Ma = 0.9 and Re_D = 40,000**
- **Halfwidth spreading rate agrees with experimental findings by Zaman for an air jet**

SJ (s > 1): Cooled-Air Jet LES I

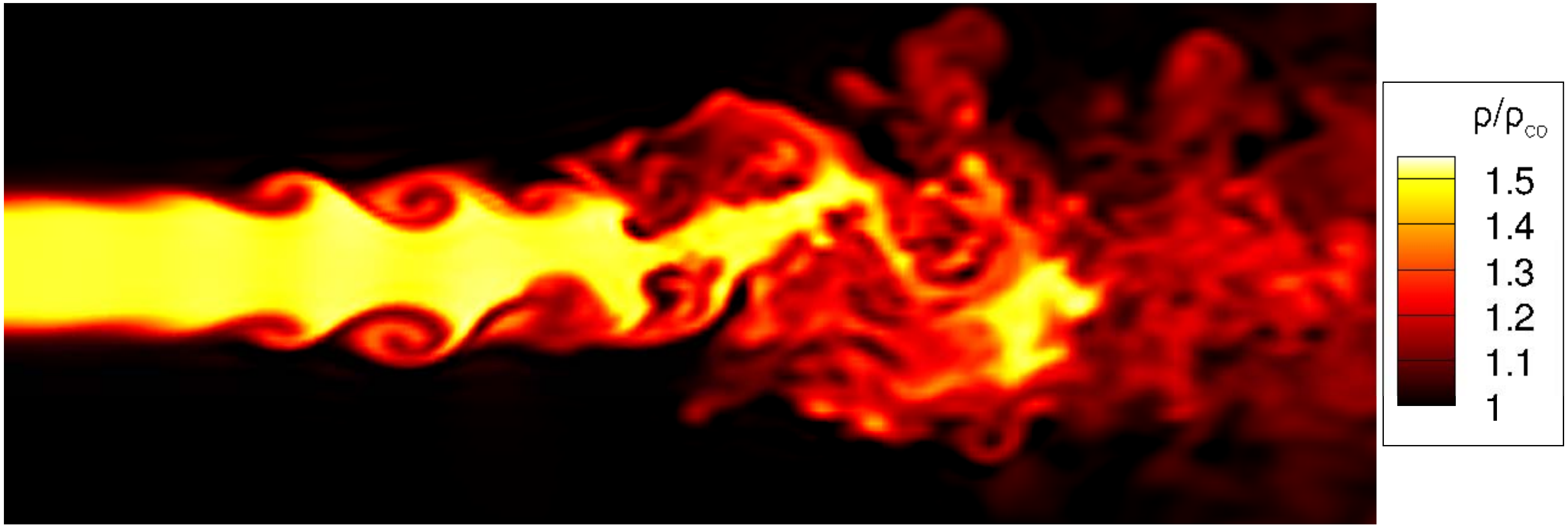

Ma = 0.6, Re$_D$ = 26,666

SJ (s > 1): Cooled-Air Jet LES II

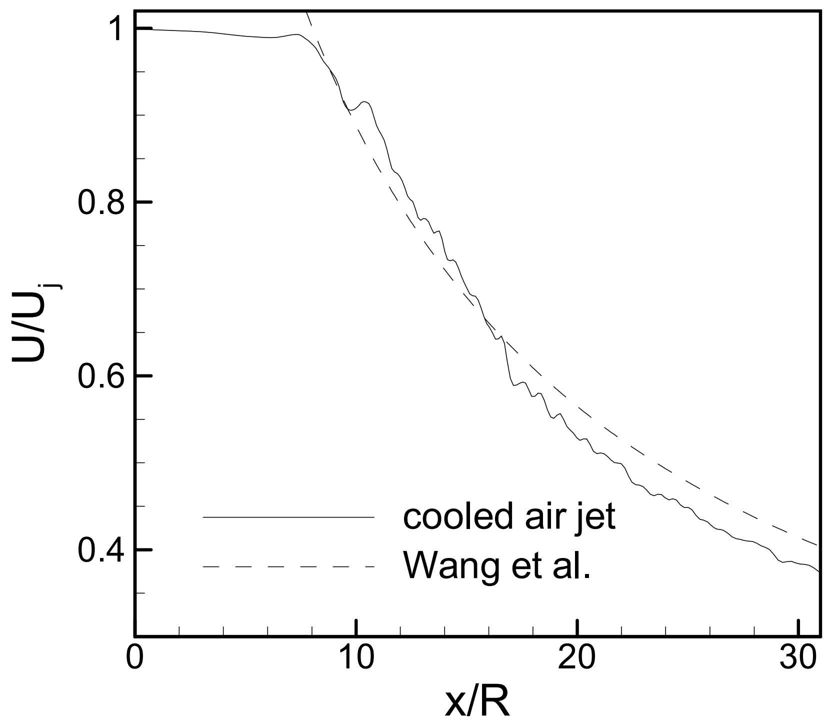

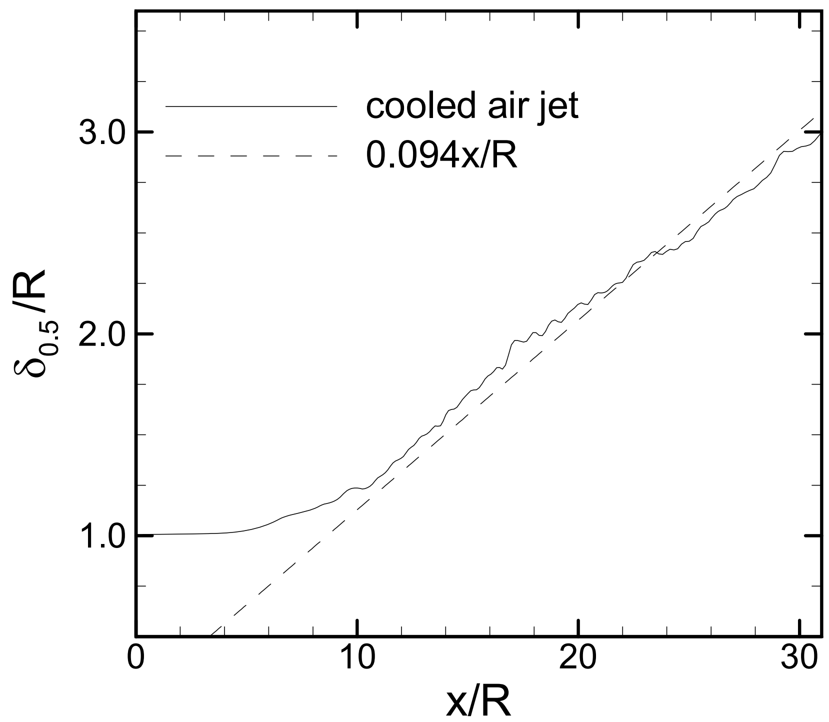

- **Centerline velocity decay fits the general scaling of Wang et al. (2008)**
- **Slope of the jet's halfwidth growth is approximately 0.094 x/R**

SJ (s > 1): Acoustic Analysis

- **Data for acoustic analyses is obtained on 18 circles forming a sphere at radius 17.5 D; on each circle 180 microphones are equidistantly distributed**

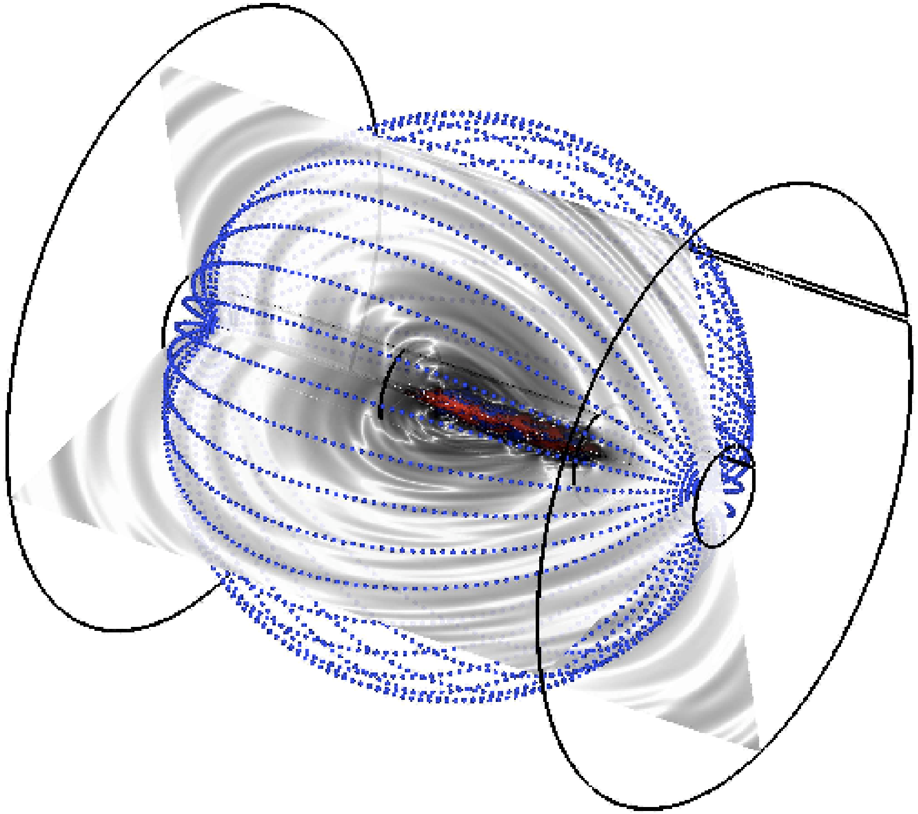

SJ (s > 1): Acoustic Pressure Field

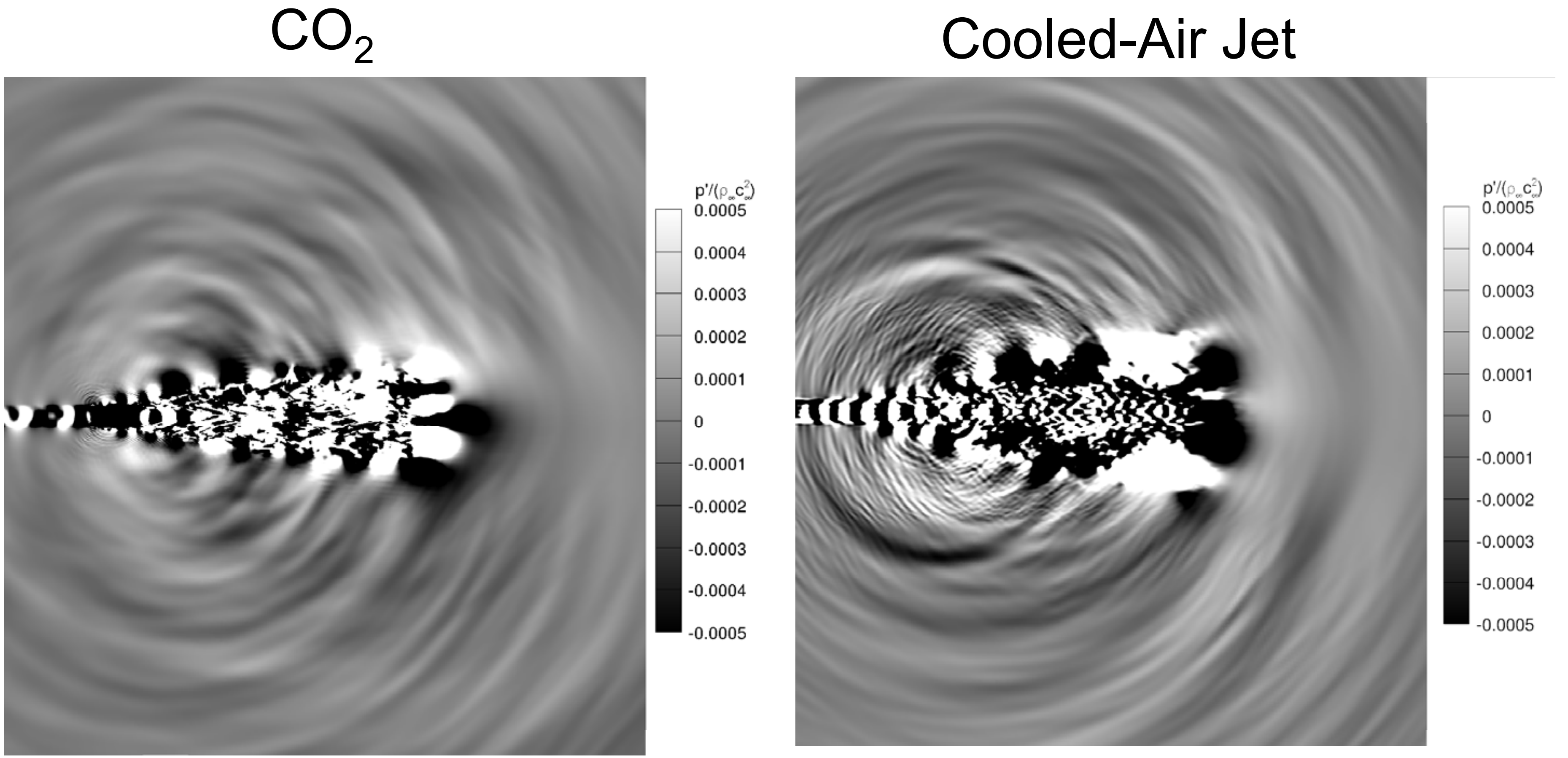

- **cooled-air jet shows larger high wavenumber content in perturbation pressure**

SJ (s > 1): OASPL

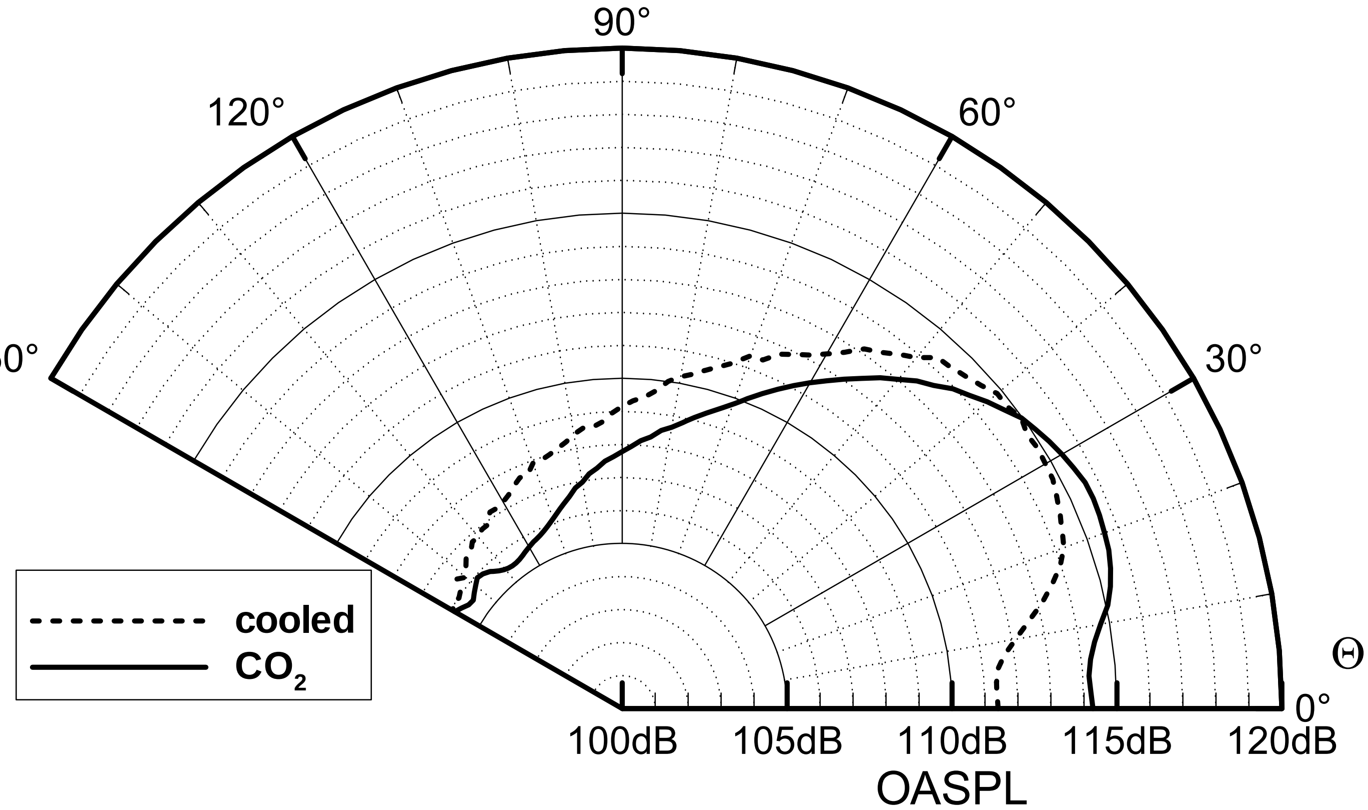

- Peak radiation varies by 1dB
- Cooled-air jet radiates at higher angles
- Largest differences occur in the sideline direction
- Overall radiation differs by max. 3dB

SJ (s > 1): Power Spectral Density I

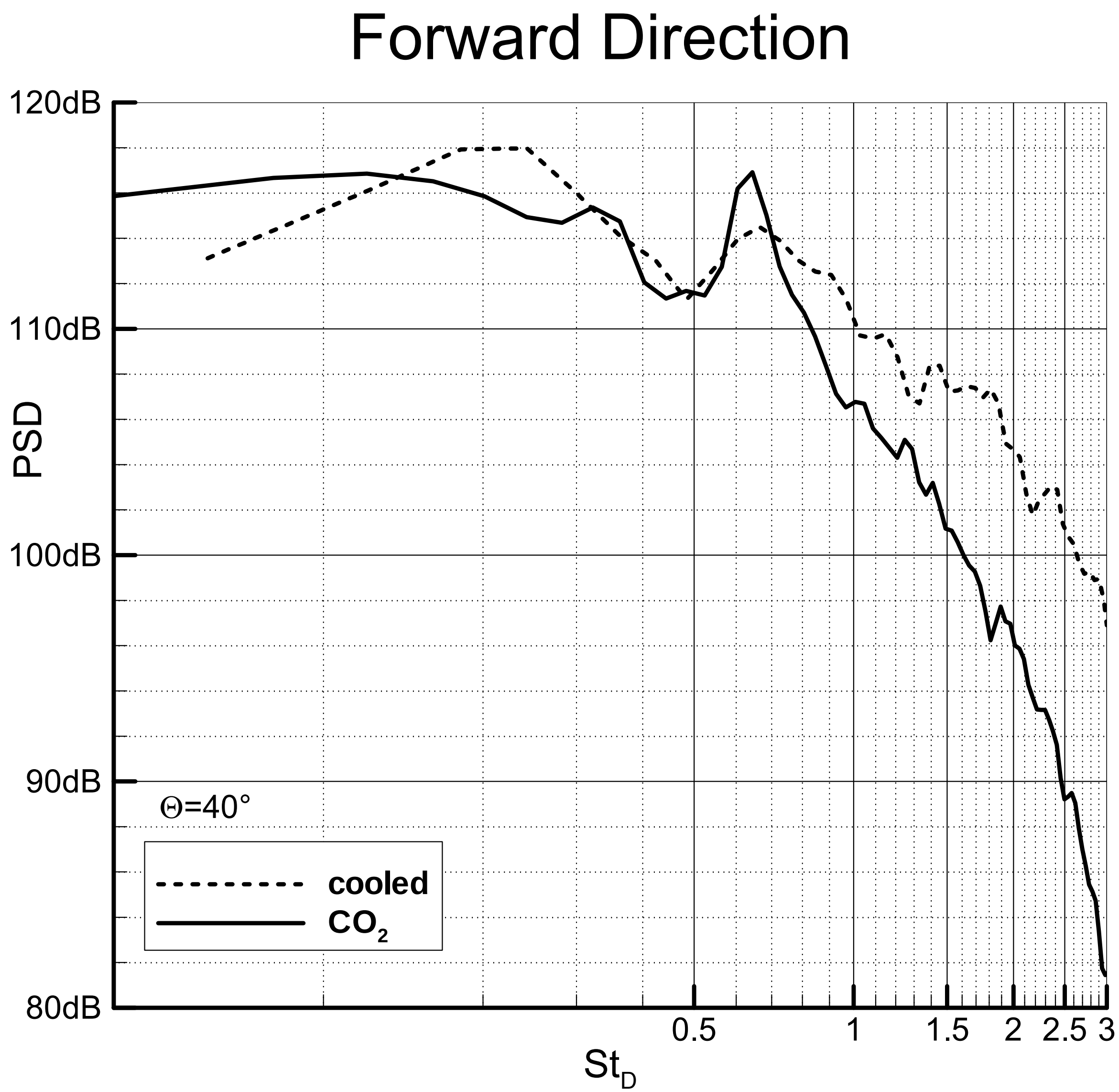

- Peak amplitude is slightly higher for the cooled-air jet
- CO_2 jet peaks at lower frequencies (St_D=0.12) than the cooled-air jet (St_D=0.24)
- A peak appears at the frequency of the shear layer instabilities

SJ (s > 1): Power Spectral Density II

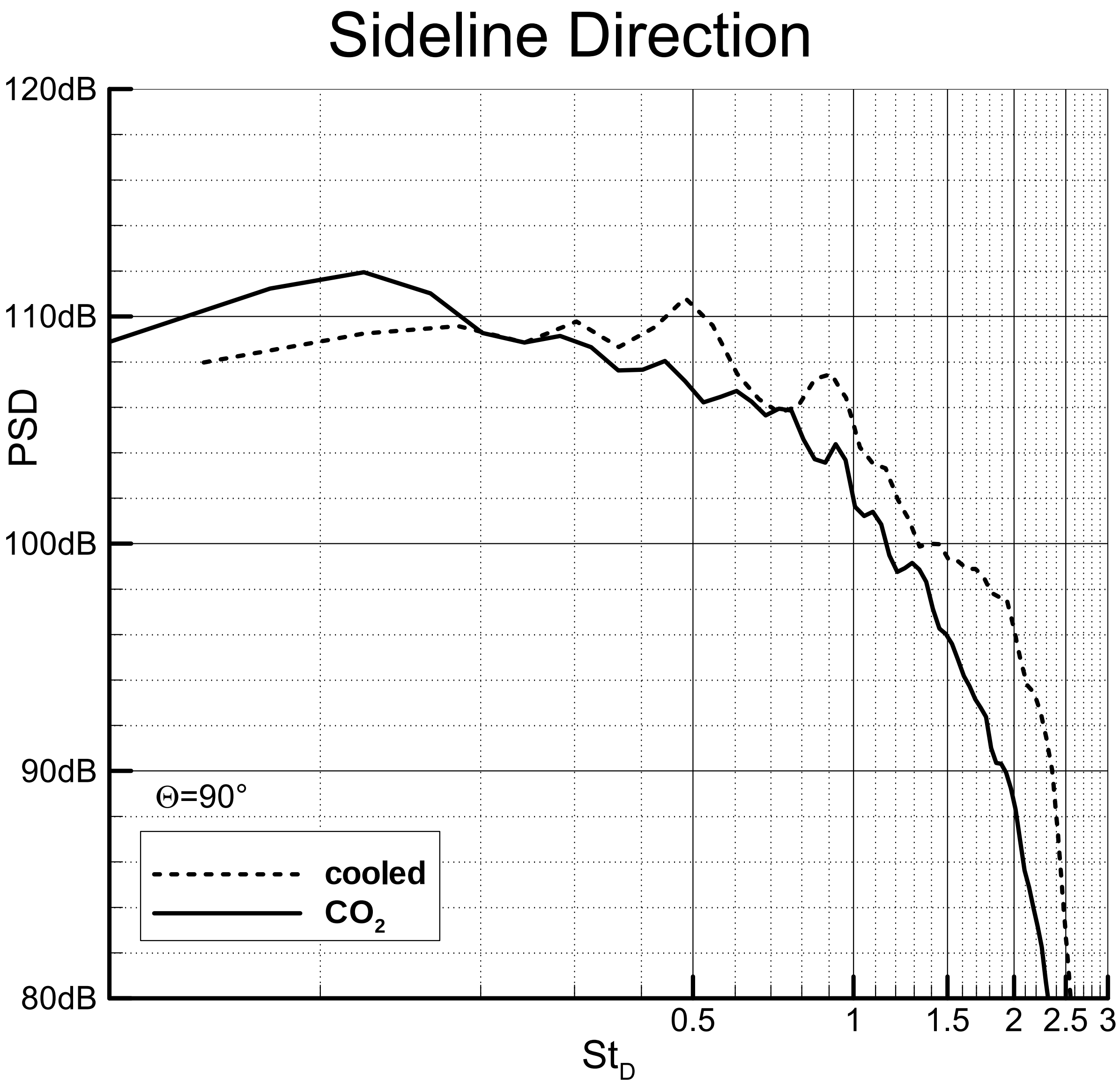

- Peak of the CO_2 jet persists at lower frequencies
- PSD slopes at higher frequencies are similar

SJ (s > 1): Power Spectral Density III

Backward Direction

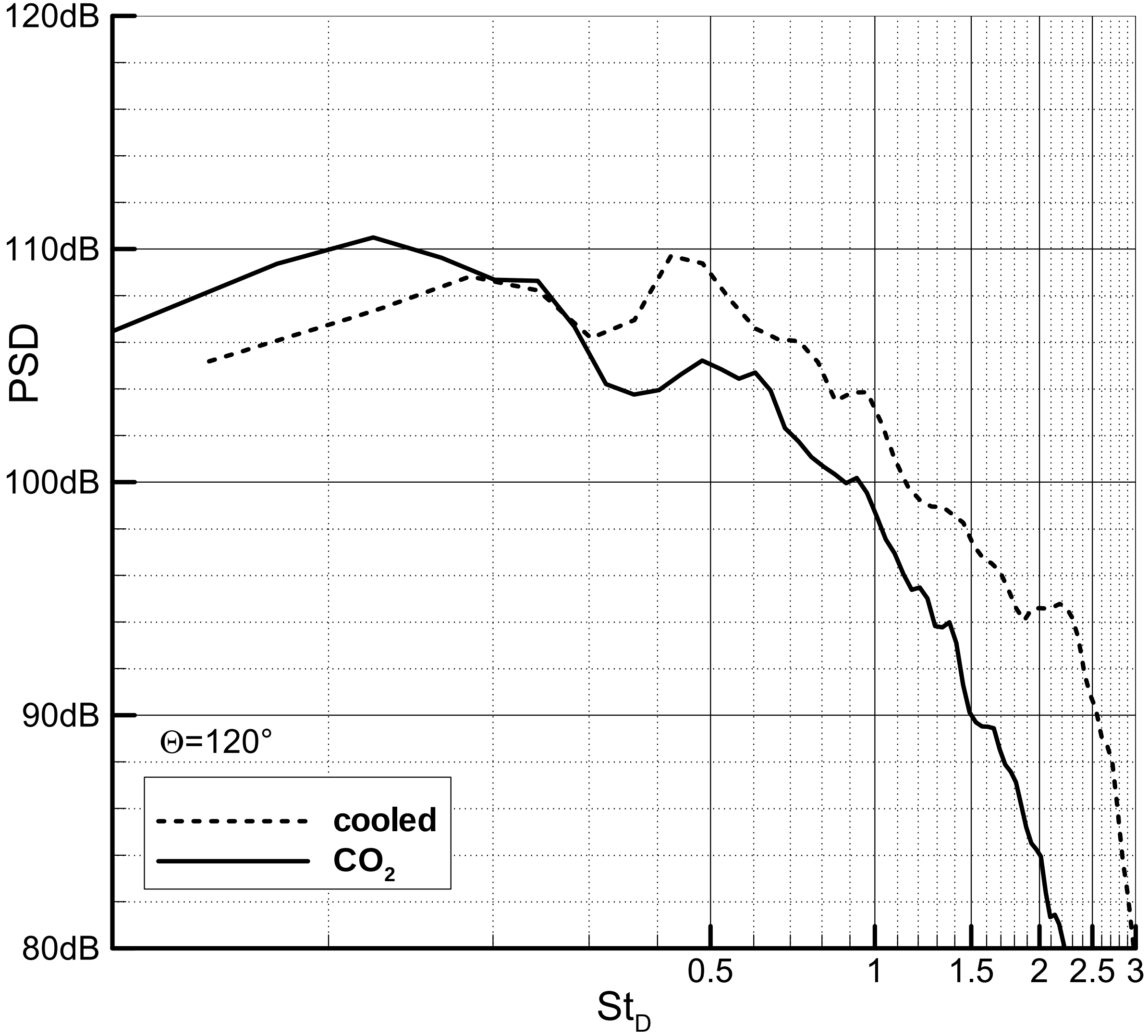

- Peak frequencies in the backward direction match
- Cooled-air jet radiates more acoustic energy
- Slopes of the spectra are similar at high frequencies

Coming Up

RWTH Aachen

Introduction

Numerical Method

- flow field
- acoustic field

Results (Fluid Mechanics, Acoustics)

- single jet
  - $\rightarrow$ s (density ratio jet/freestream) = 1
  - $\rightarrow$ s > 1
  - $\rightarrow$ s < 1
- coaxial jet

Conclusions

Numerical Method

Motivation

Physics:

- anything different compared to s > 1 jets ?
  → stability ?

Numerics:

- impact of filter width on SPL

SJ (s < 1): Numerical Method

- Fully parallelized compressible NS-solver
- 6th-order explicit SBP-DRP-SAT and compact schemes for spatial derivatives (Johansson (2004)) and LDD-Runge Kutta of fourth order (Hu et al. (1996)) for time integration
- Nonreflecting boundary conditions (Lodato et al. (2008)) and Grid stretching + spatial filtering in sponge-zone
- Centerline treatment after Constantinescu & Lele (2002), Mohseni & Colonius (2002)
- Initial velocity profile for round jet (similar in plane jet):

$$u = u_{co} + \frac{1}{2}(u_j - u_{co})\left(1 - \tanh\left[\left(\frac{r}{r_j} - \frac{r_j}{r}\right)\frac{1}{4\delta_{\theta 0}}\right]\right)$$

temperature determined by Crocco-Busemann relation

- Dynamic Smagorinsky subgrid model + artificial dissipation for the low s cases (Fiorina & Lele (2007))

SJ (s < 1): Inflow Perturbations

- Transition to turbulence triggered by combination of random forcing and precursor simulation:
  - Solenoidal broadband perturbations, with prescribed energy spectrum of the form $E(k) \propto k^4 \exp[-(k/k_o)^2]$ convected into domain, using low amplitudes
  - Precursor simulations of annular and plane mixing layers were performed
    - Smaller initial momentum thickness due to temporal growth
    - Square root of TKE monitored until its non-dimensional value $\sqrt{(u')_1^2 + (u')_2^2 + (u')_3^2}$ was of the order of 0.05 ...
    - ... and mean profiles agreed with inlet jet profiles
    - Fast jet development, compares well with Wang et al. (2008)

SJ (s < 1) Parameters of Variable Density Jets

RWTH Aachen

Case	Re_D	$D/\delta_{\theta 0}$	s	L_x	L_r	L_θ	$n_x \times n_r \times n_\theta$
LES014	7000	27	1/7	60	16	2π	320×120×64
DNS014	7000	54	1/7	52	14	2π	1024×320×256
DNS FR100	21000	80	1	45	12	2π	2560×640×320
DNS FR152	21000	80	1,52	45	12	2π	2560×640×320

Mach number Ma = 0.3 based on jet radius r_j and velocity U_j; simulations possess a constant inlet momentum flux (Ricou et al. (1961)), Ruffin et al. (1994) $\rightarrow$ Reynolds numbers differ (Foysi et al. (2010))

SJ (s<1): Visualization of an s = 1.52 jet

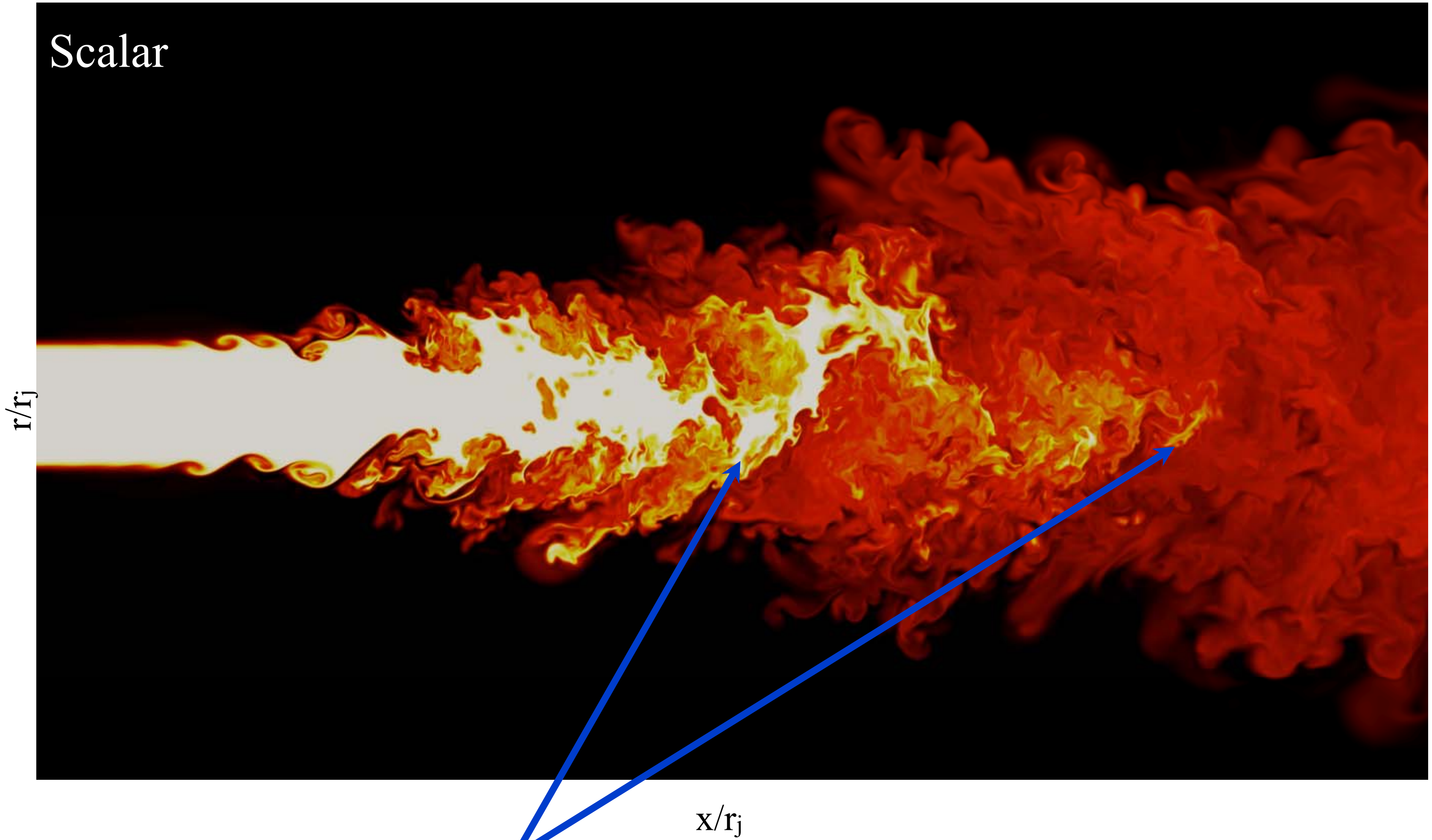

High concentration found far downstream

SJ (s<1): Visualization of an s = 0.14 jet

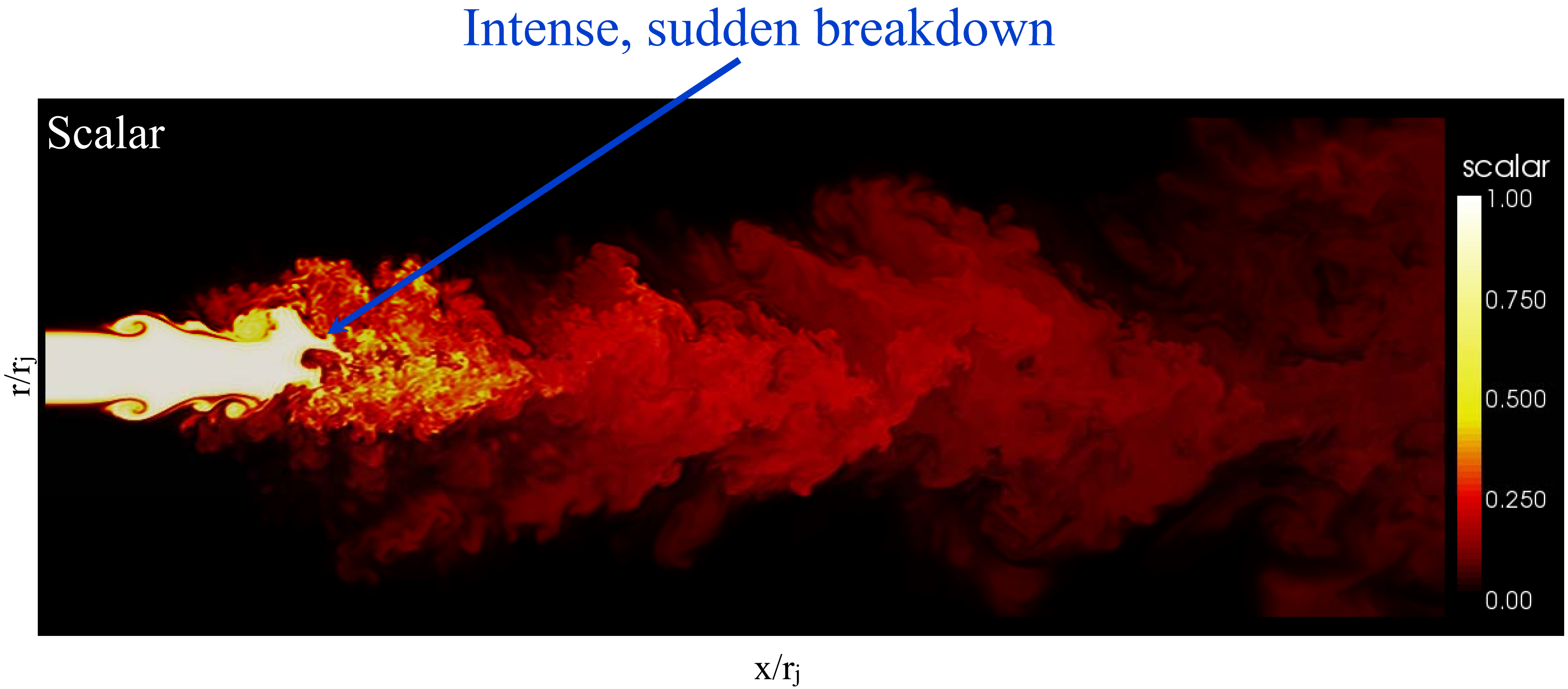

- Intense potential core collapse indicates a profound influence on the radiated sound spectrum, since it is well known that there is a close link between turbulence in the core region and the sound generation (Lighthill (1954))

SJ (s<1): DNS Mean Vel. at Various s I

- Good agreement of centerline velocity decay with Chen & Rodi (1980) and Wang et al. (2008), Amielh et al.

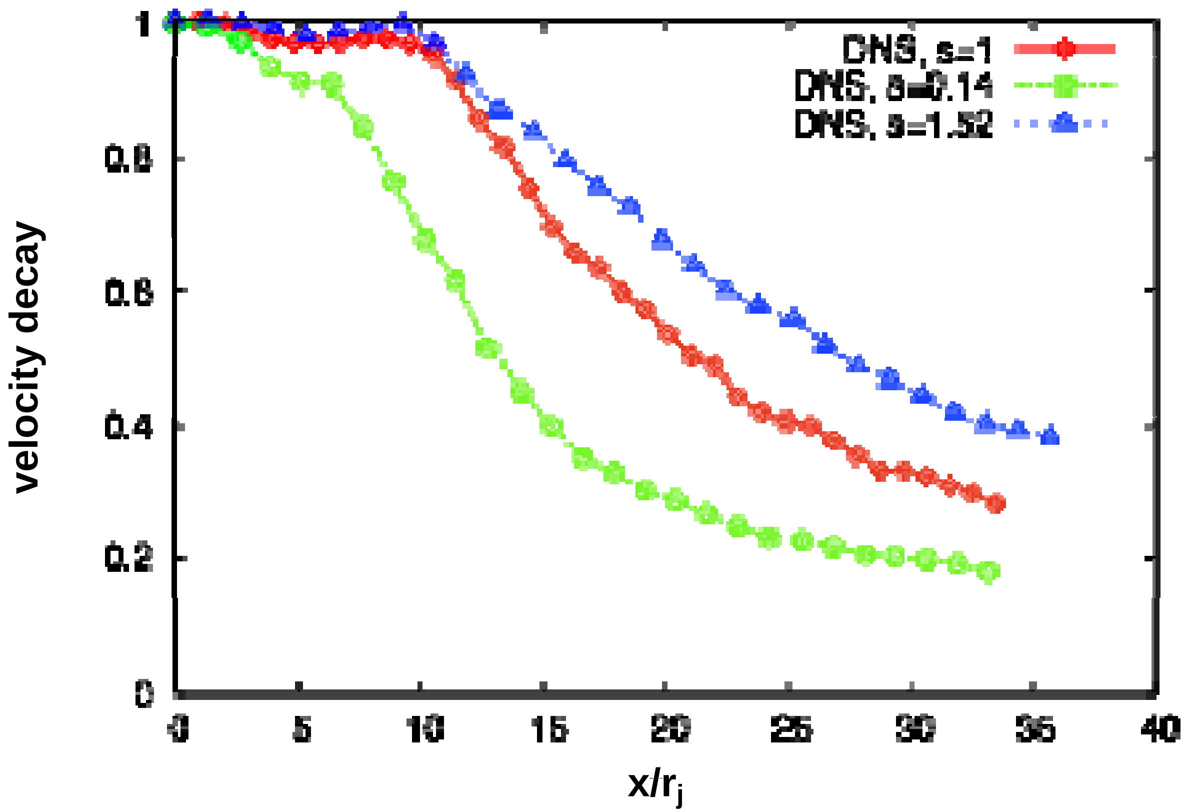

SJ (s<1): LES Mean Vel. at Various s II

- Good agreement of centerline velocity decay with Chen & Rodi (1980) and Wang et al. (2008), Amielh et al.
- Self-similar behavior for $u-u_{co}$ observed, irrespective of density ratio
- Round jet mean velocity follows exponential decay law $\exp[-(r/r_h)^2 \ln 2]$

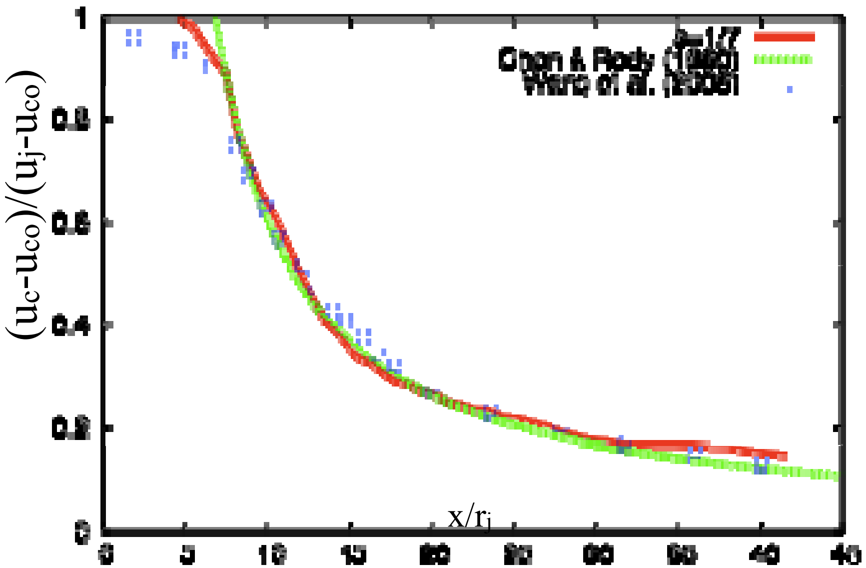

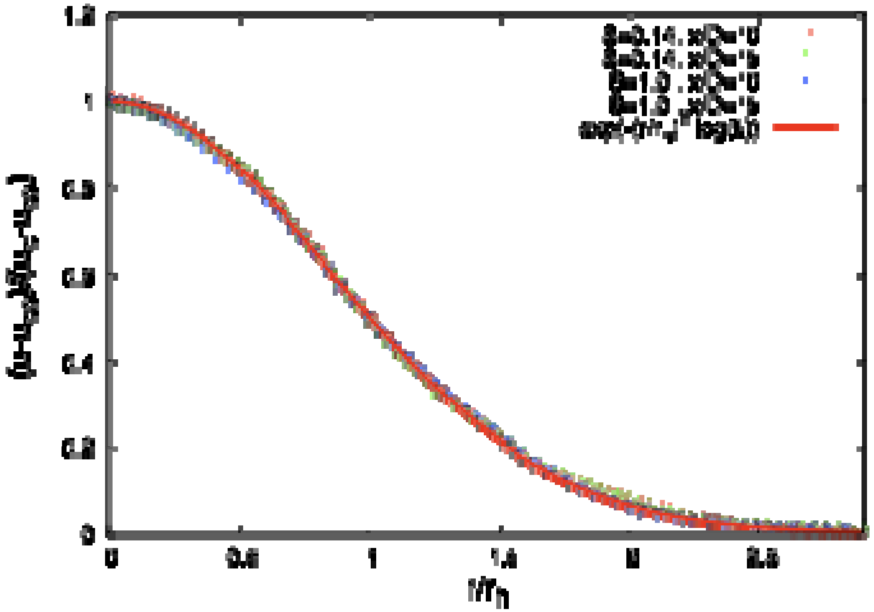

SJ (s<1): s=0.14 Global Inst. via LES

- For a density ratio of s=1/7 huge **self-sustained oscillations** (Sreenivasan e… …ed to stabilize simulation (Fi…
- Velocity powe… …ant frequency + overtones up…

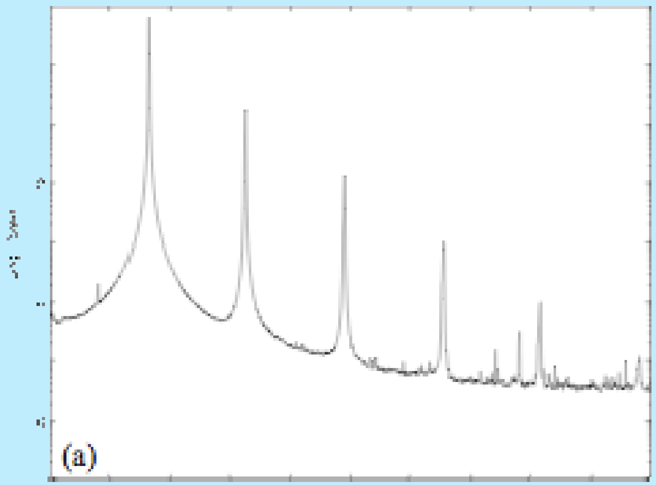

Experiment, Hallberg & Strykowski (2006)

St

$St_D=$

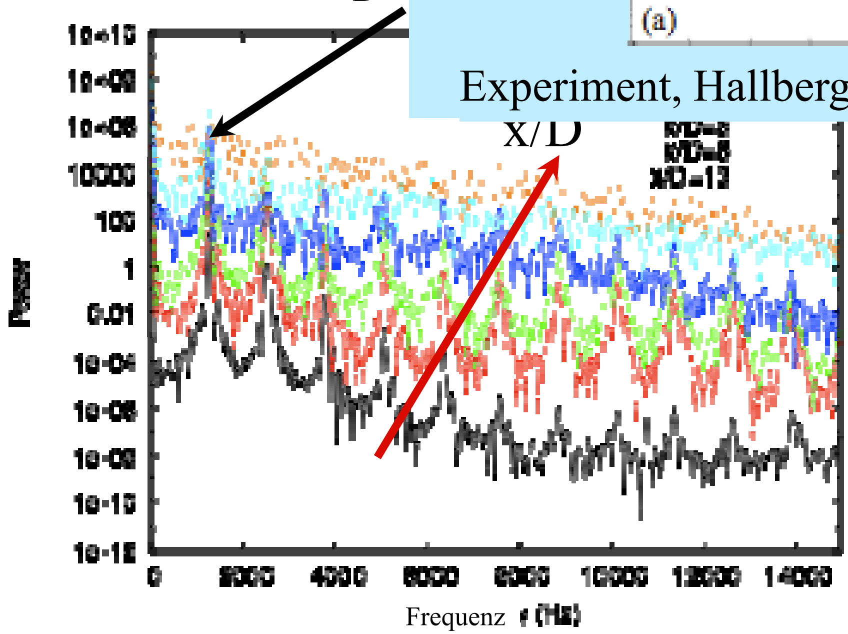

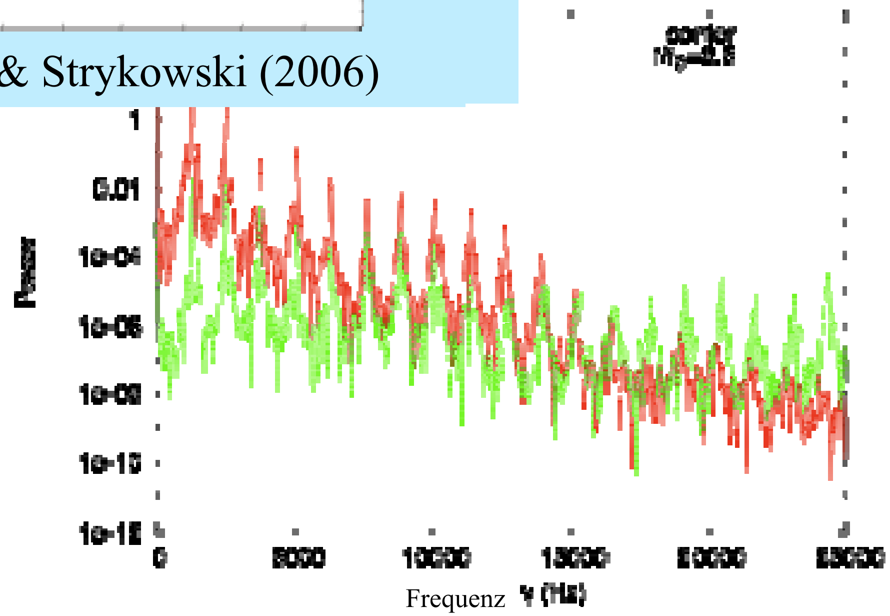

SJ (s<1): s=0.14 Global Instability via DNS

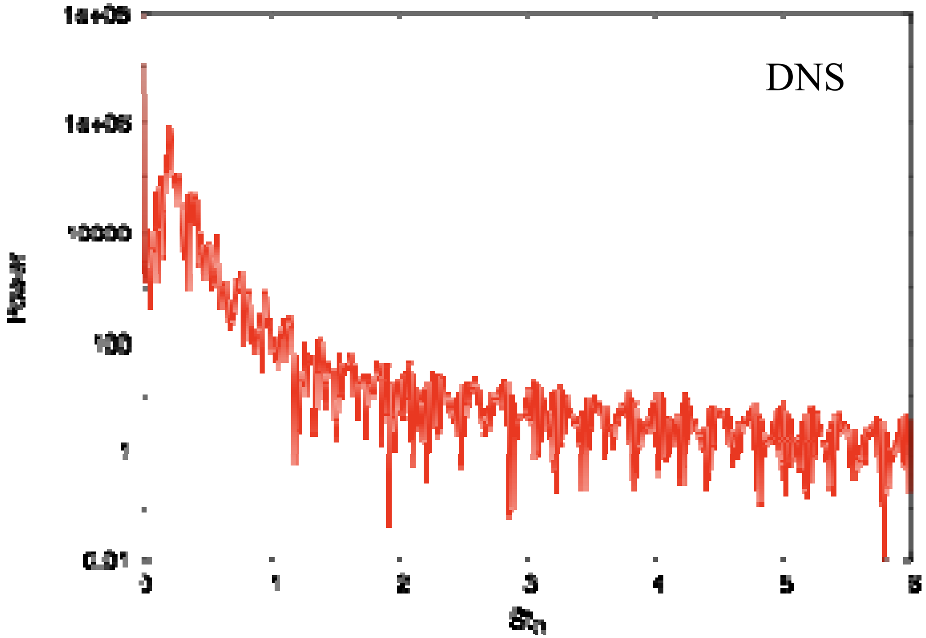

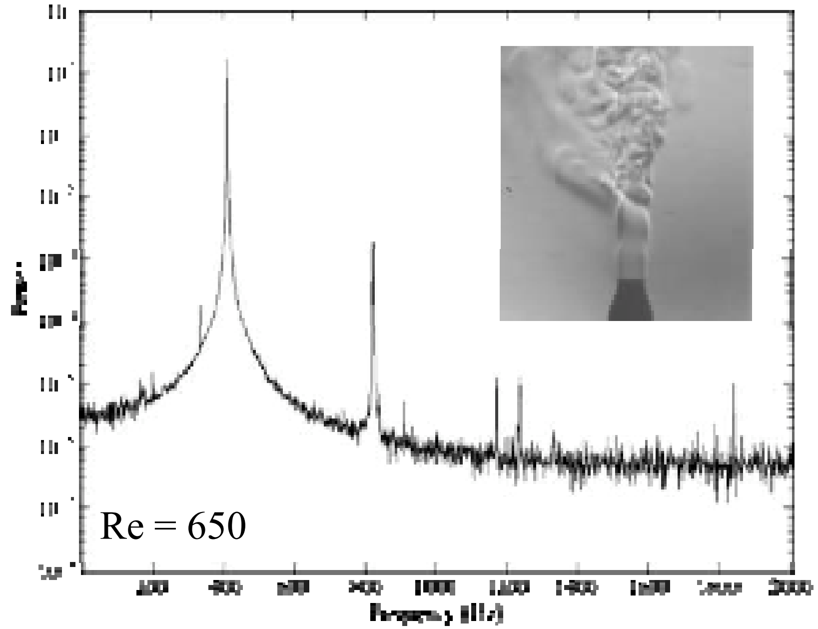

Experiment, Hallberg & Strykowski (2006)

- DNS shows global instability mode with $St_D = 0.27$
- DNS showed less distinct peak compared to LES; higher Strouhal number due to smaller initial shear layer thickness!

SJ (s<1): Comparison with Exp. Data

- Strouhal numbers of St_D=0.22 (LES) and St_D=0.27 (DNS)
- Excellent agreement with experimental data. Influence on sound field?

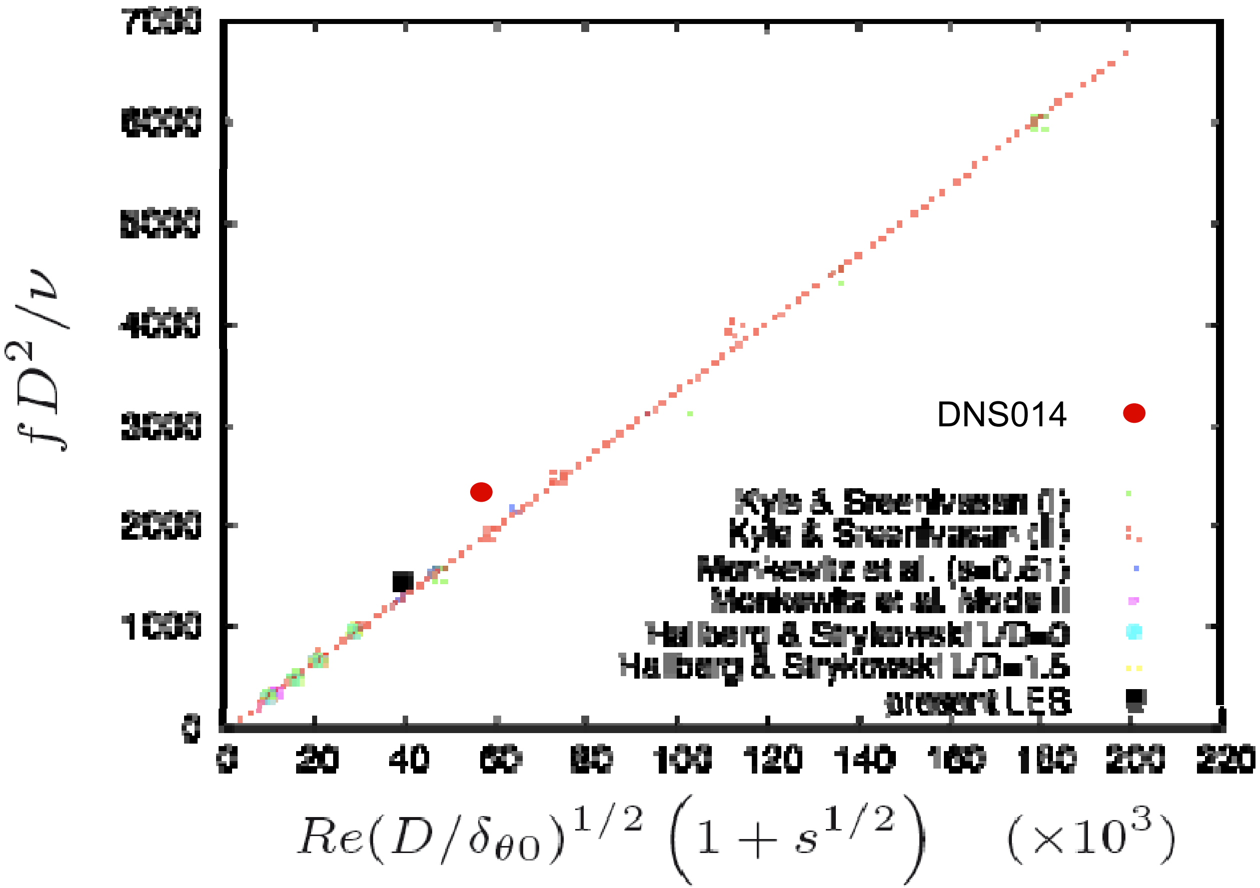

SJ (s<1): Spectral Analysis

Data Processing

Total 1500 samplings (LES)

Total 900 samplings (DNS)

Δt_s = 0.125 D/U_j (DNS)

Δt_s = 0.09 D/U_j (LES)

Window function

$$w(t) = \frac{1}{2}\left[\tanh\left(5\frac{t-t_1}{t_1-t_0}\right) - \tanh\left(5\frac{t_f-t}{t_f-t_2}\right)\right]$$

Azimuthal mode decomposition

$$q_n = \sum_{j=0}^{N-1} q(z,t,r,\theta_j)e^{-in\theta_j}$$

DNS fields filtered: SGS-TKE
DNS014f1 9% of TKE
DNS014f2 21% of TKE
DNS014f3 28% of TKE

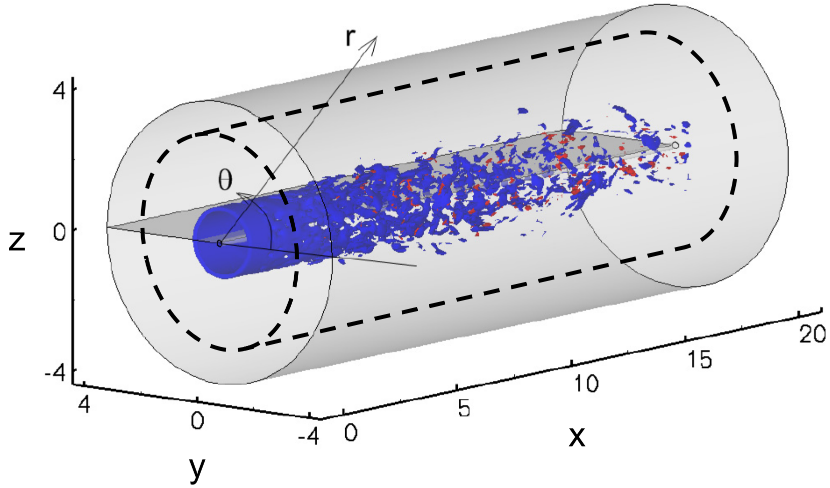

Source domain extended

$0 \le x/r_j \le 37$ $0 \le r/r_j \le 8$

APE domain used same grid as DNS/LES, max. $\Delta r = 0.2 r_j$ from

$-40 \le x/r_j \le 80$ $0 \le r/r_j \le 70$

$St_D \approx 2.5 - 6$

Up to 250 Million grid points

SJ (s<1): Spectral Analysis of DNS Data I

Fourier Transform of Noise Source (Axial Location / Frequency)

$$\hat{q}(\mathbf{x},\omega) = \int_{-\infty}^{\infty} q(\mathbf{x},t)\, e^{-i\omega t}\, dt$$

$r=0.1r_j$

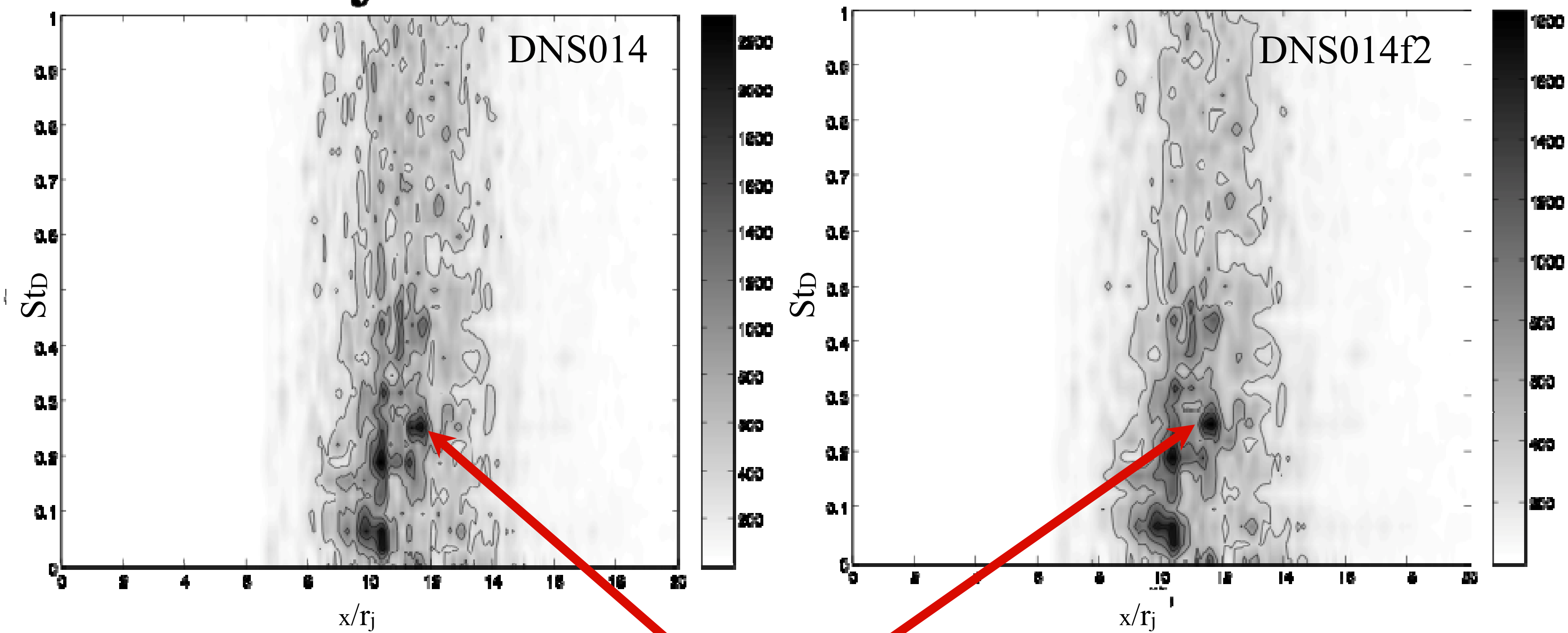

Global mode instability

SJ (s<1): Spectral Analysis of DNS Data II

Fourier Transform of Noise Source (Axial Location / Frequency)

$$\hat{q}(\mathbf{x},\omega) = \int_{-\infty}^{\infty} q(\mathbf{x},t)\, e^{-i\omega t}\, dt$$

r=0.5r_j

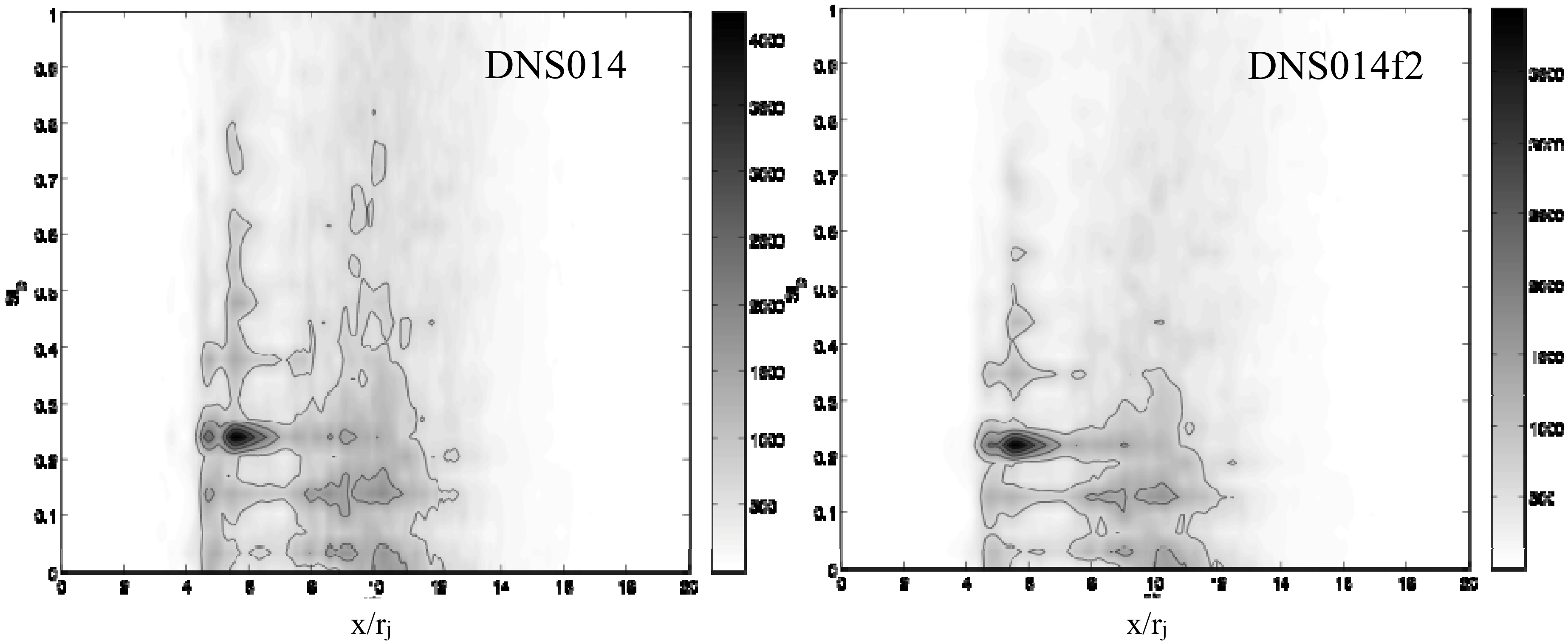

SJ (s<1): Spectral Analysis of DNS Data III

Fourier Transform of Noise Source (Axial Location / Frequency)

$$\hat{q}(\mathbf{x},\omega) = \int_{-\infty}^{\infty} q(\mathbf{x},t)\, e^{-i\omega t}\, dt$$

r=r_j

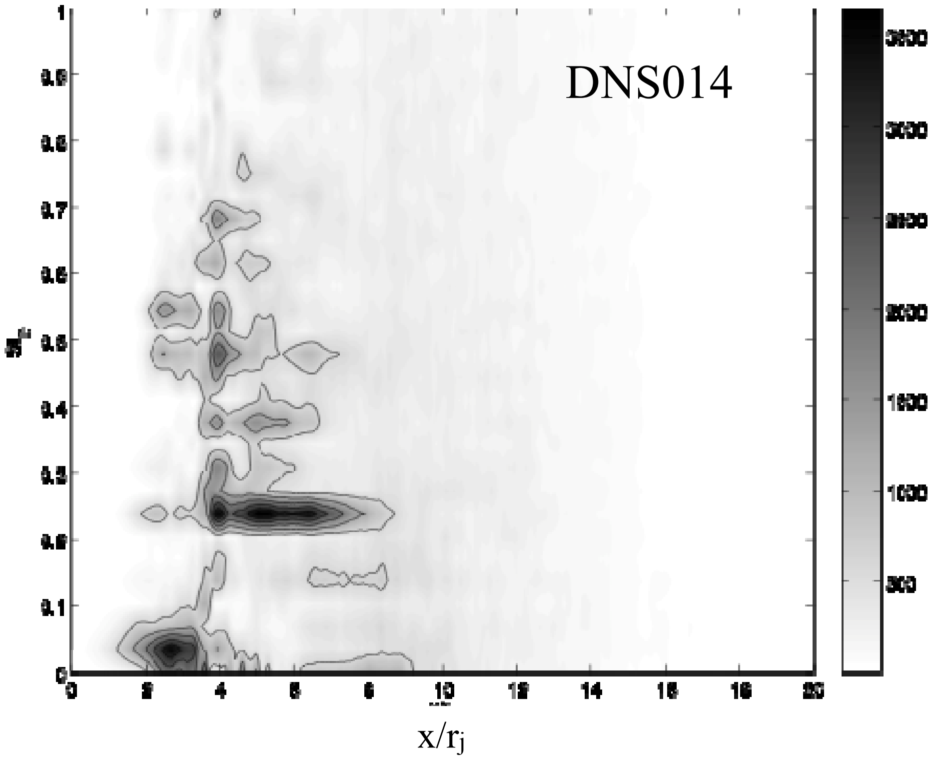

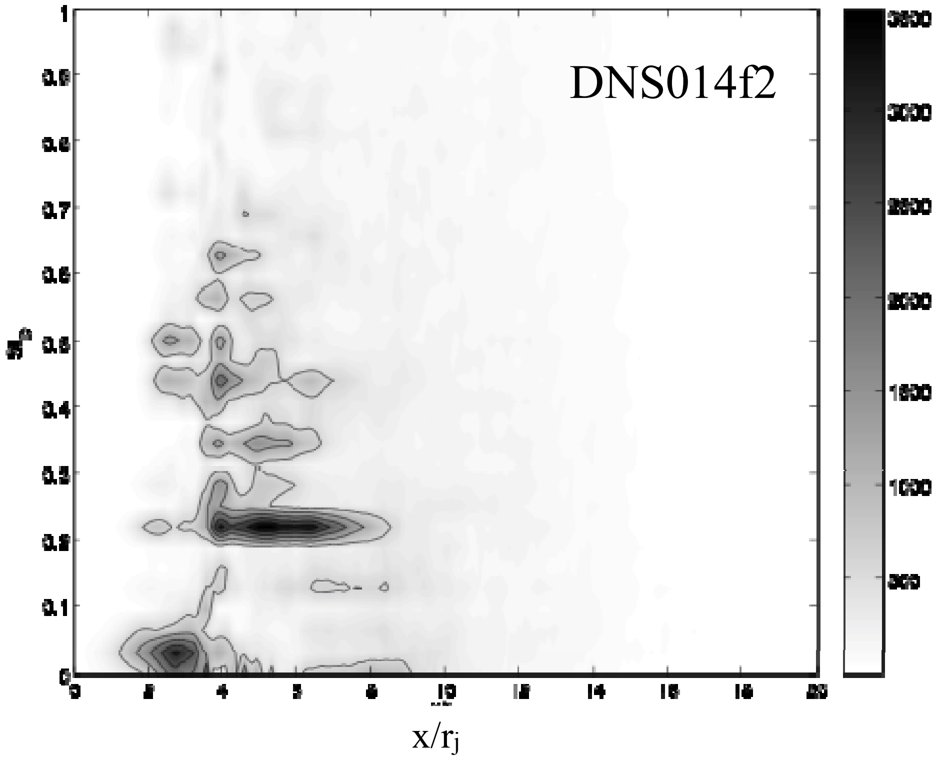

- Global instability dominates PSD at all radii

SJ (s<1): Impact of Filter Width on SPL

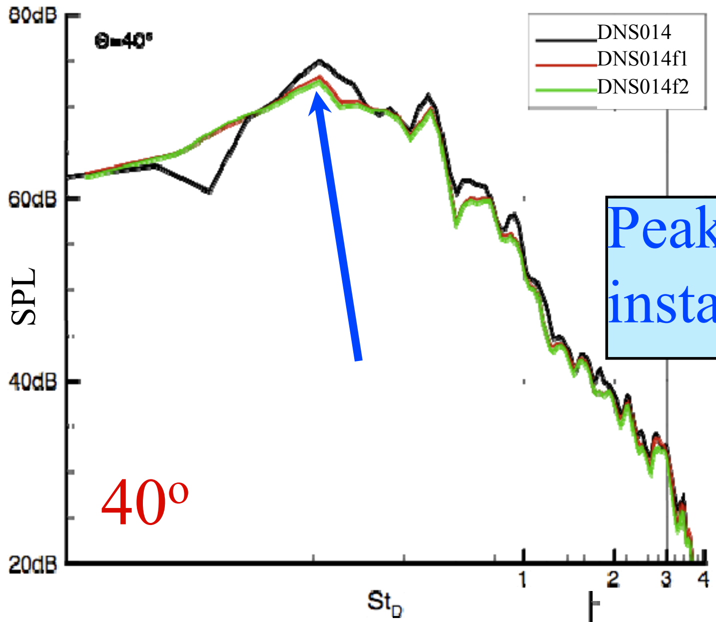

Peak at global instability St_D

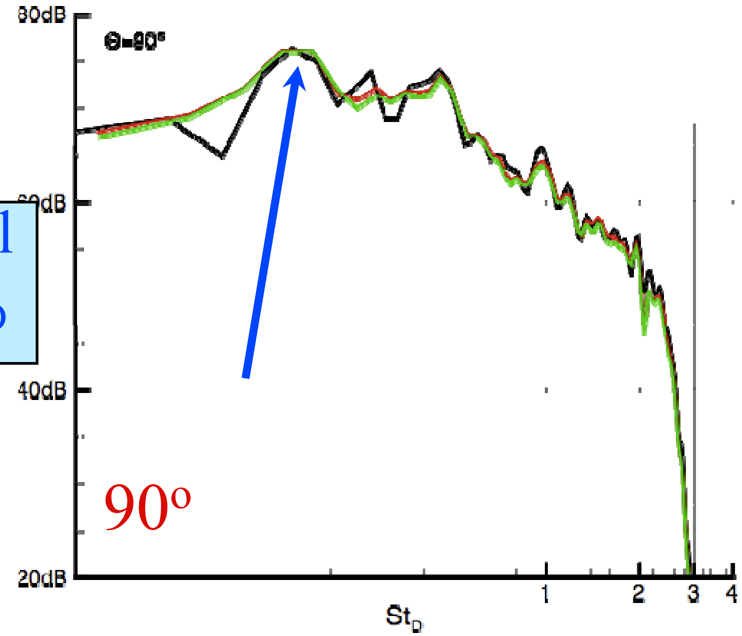

SPL(ω) (in dB per radian freq.)

$$= 10\log_{10}\frac{S_{pp}(\omega)}{p_{\mathrm{ref}}^2}$$

$$S_{pp}(\omega) = \int_{-\infty}^{\infty} \langle p'(t)p'(t+\tau)\rangle e^{i\omega\tau}\,\mathrm{d}\tau.$$

$$p_{\mathrm{ref}} = 20\,\mu\mathrm{Pa}$$

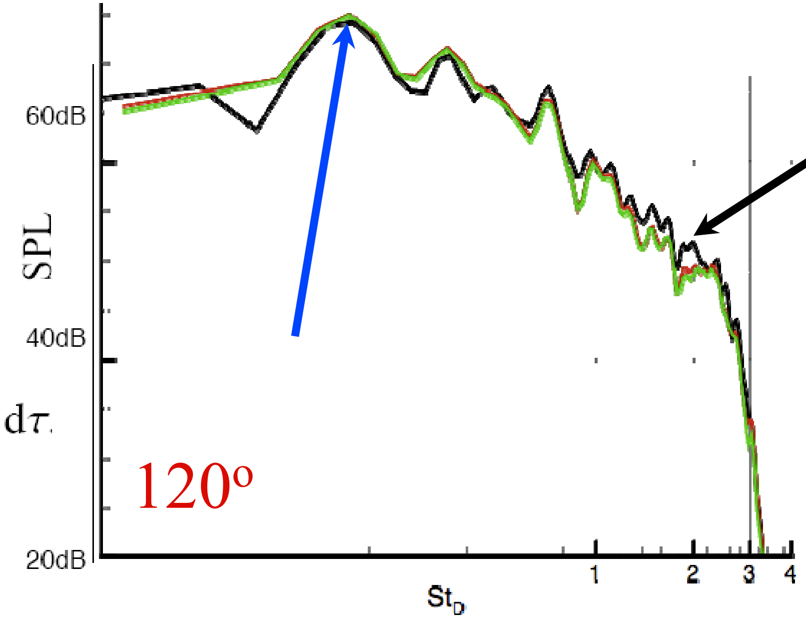

SJ (s<1): Impact of Filter Width on Ac. Field

- DNS014 (left) vs. DNS014f2 (right)

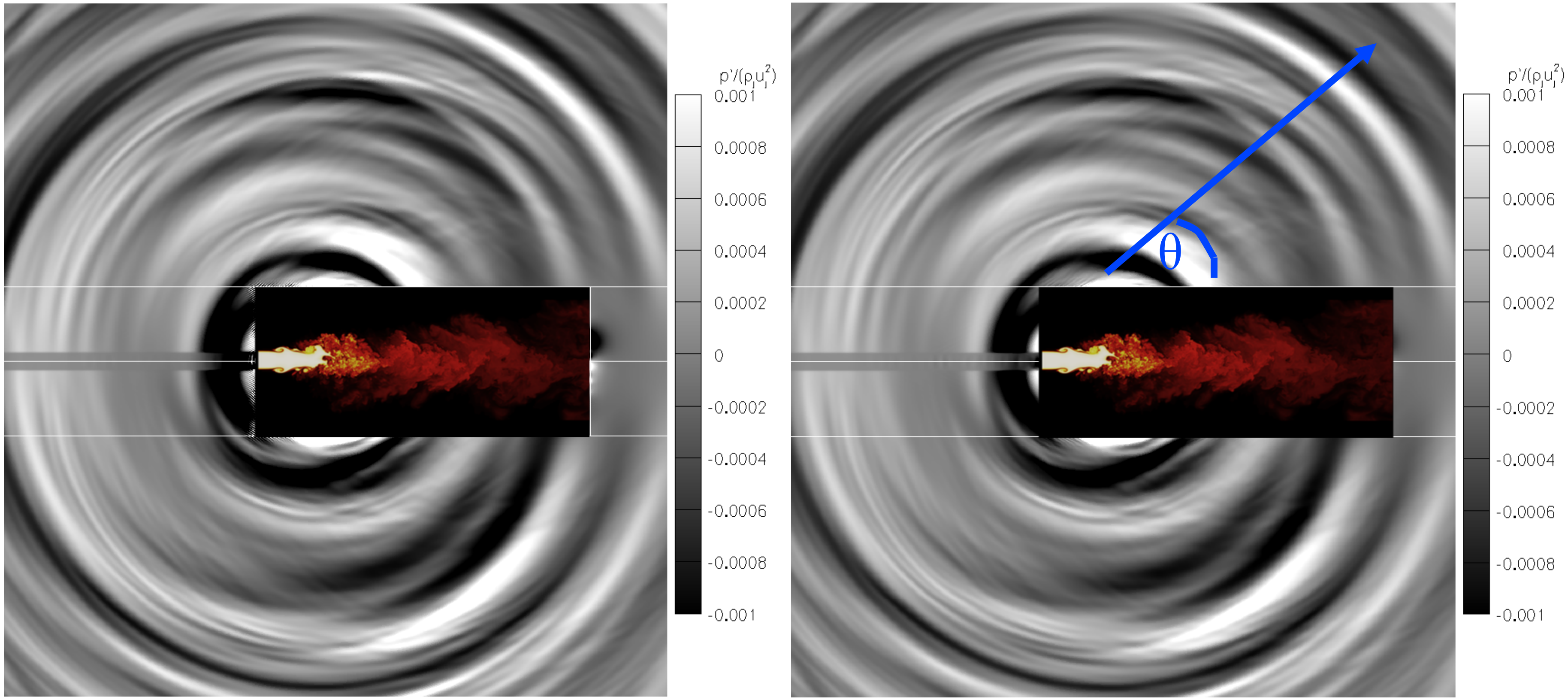

- 120-500 Million grid points on 4096-8192 processors on Blue-Gene/P at Jülich Supercomputing Center
- Similarity solution used to extend mean field in the streamwise direction

SJ (s<1): DNS – LES SPL Comparison

- Filtered DNS, DNSf3 removing 28% of the TKE
- Finer LES014: 512 x 160 x 64 grid points (x, r, θ)

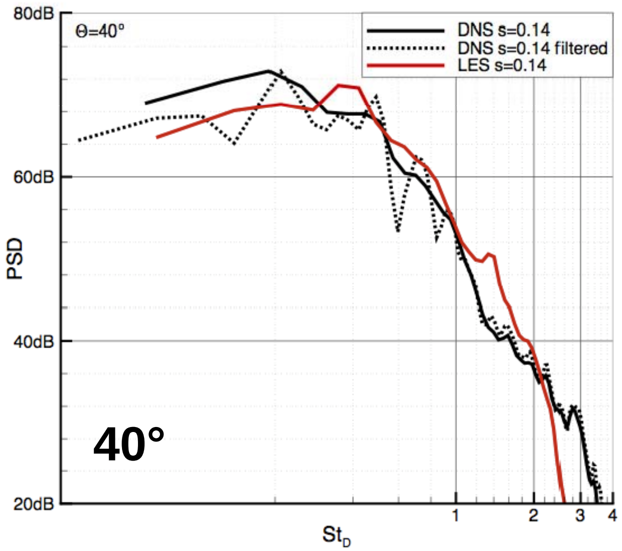

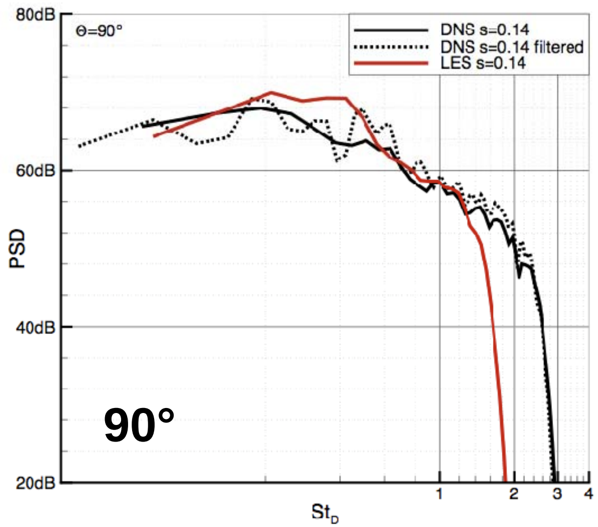

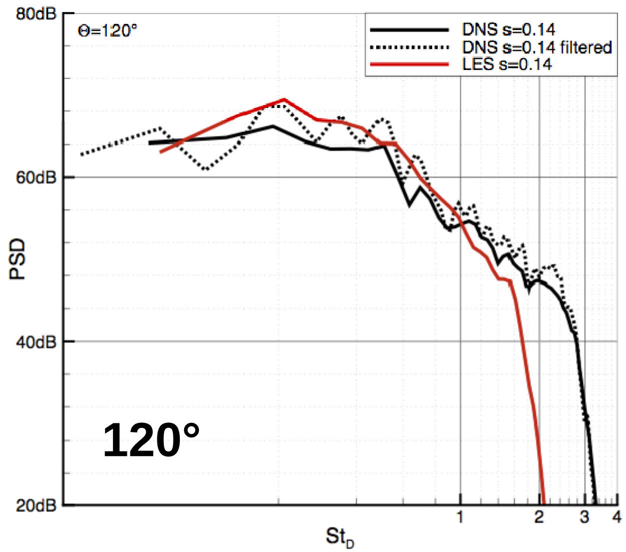

SJ (s<1): DNS – LES OASPL Comparison

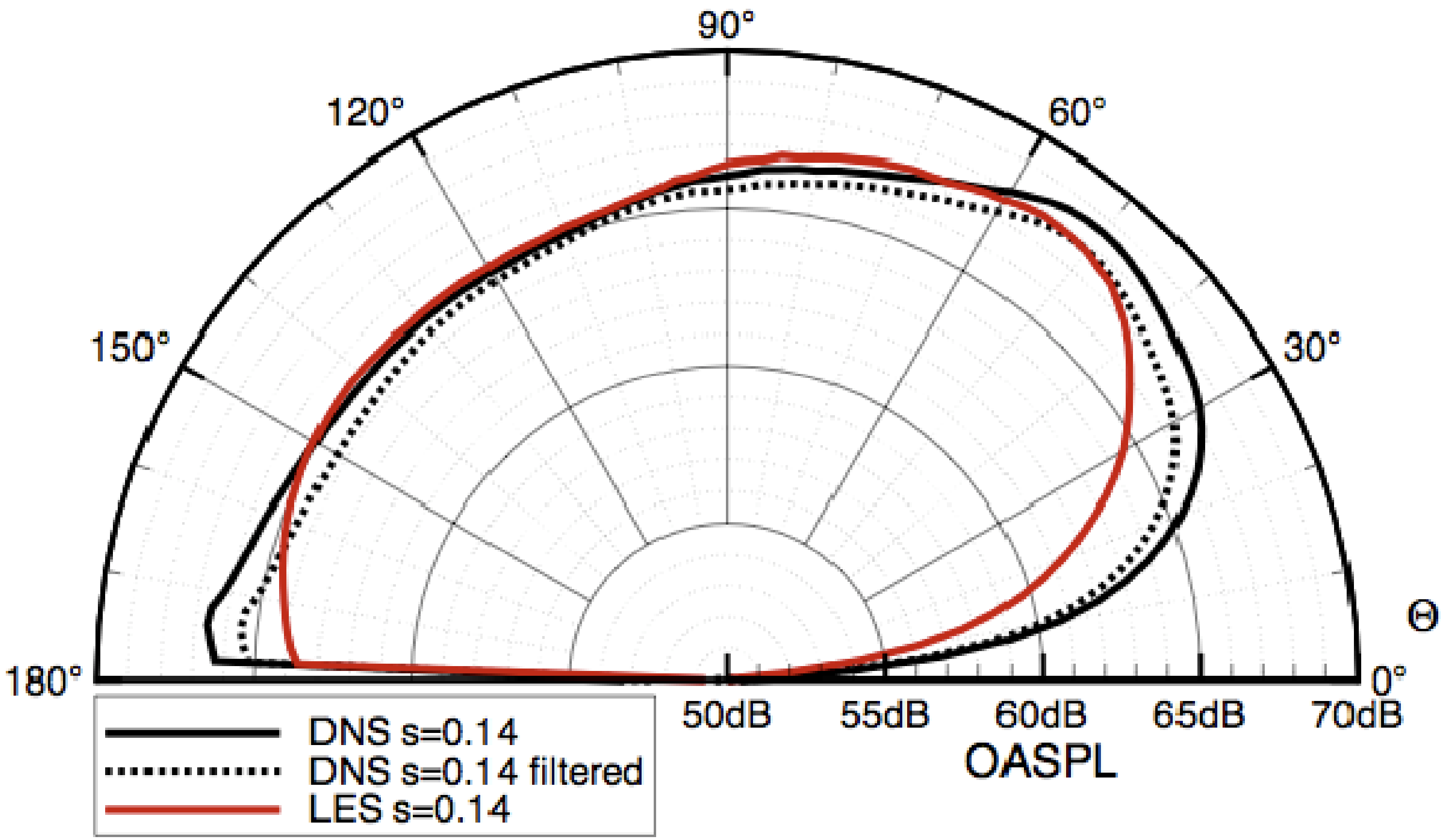

SJ (s<1): DNS – LES SPL Comparison

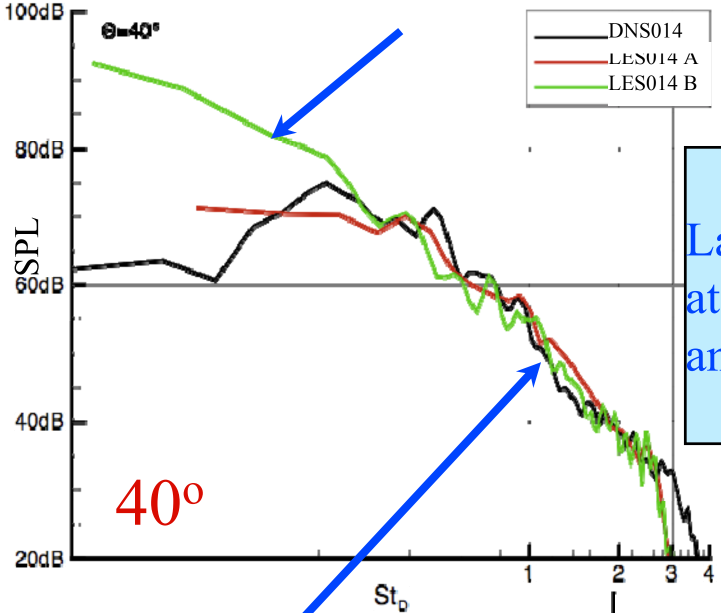

Large PSD increase at low ST_D. Is there an explanation?

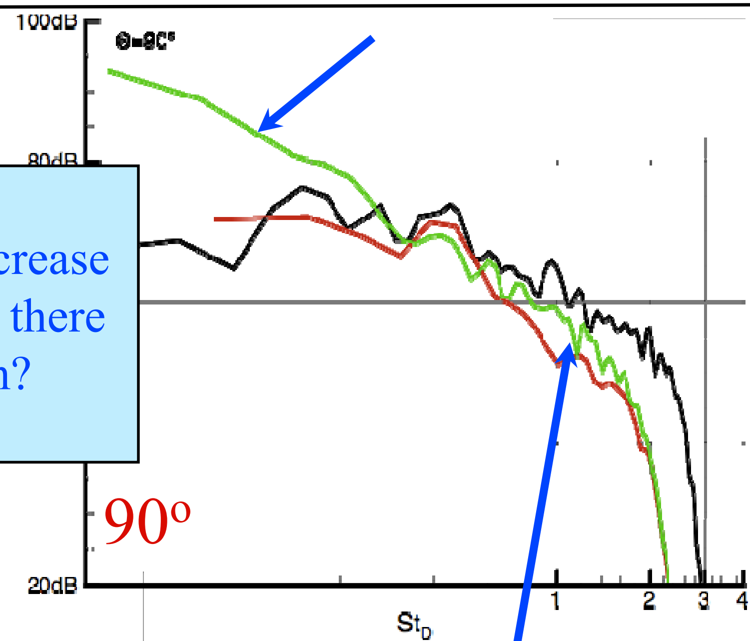

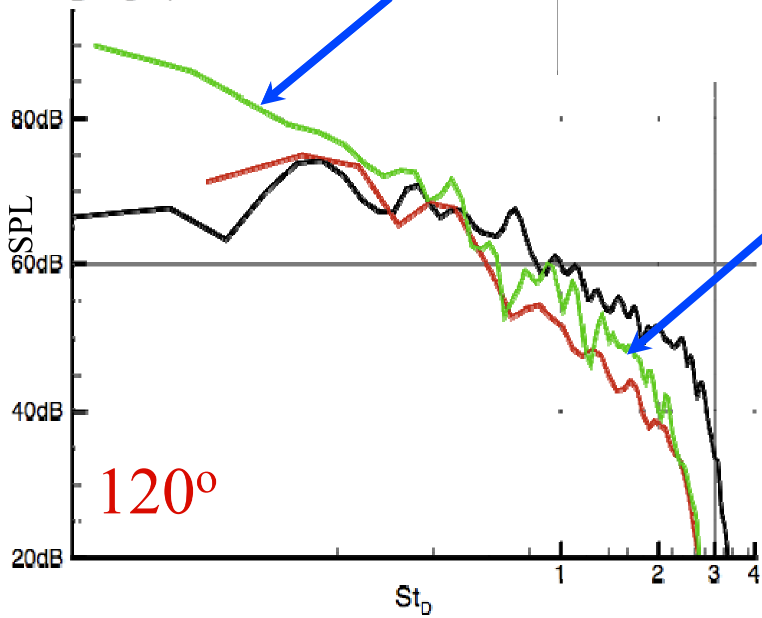

Forward radiation dominated by large structures near centerline: resolved by LES!

5-12dB difference, sideline radiation mainly due to small scales near shear layer: not resolved by LES!

SJ (s<1): Microphone Time Series

- Sudden strong pressure increase in the far field

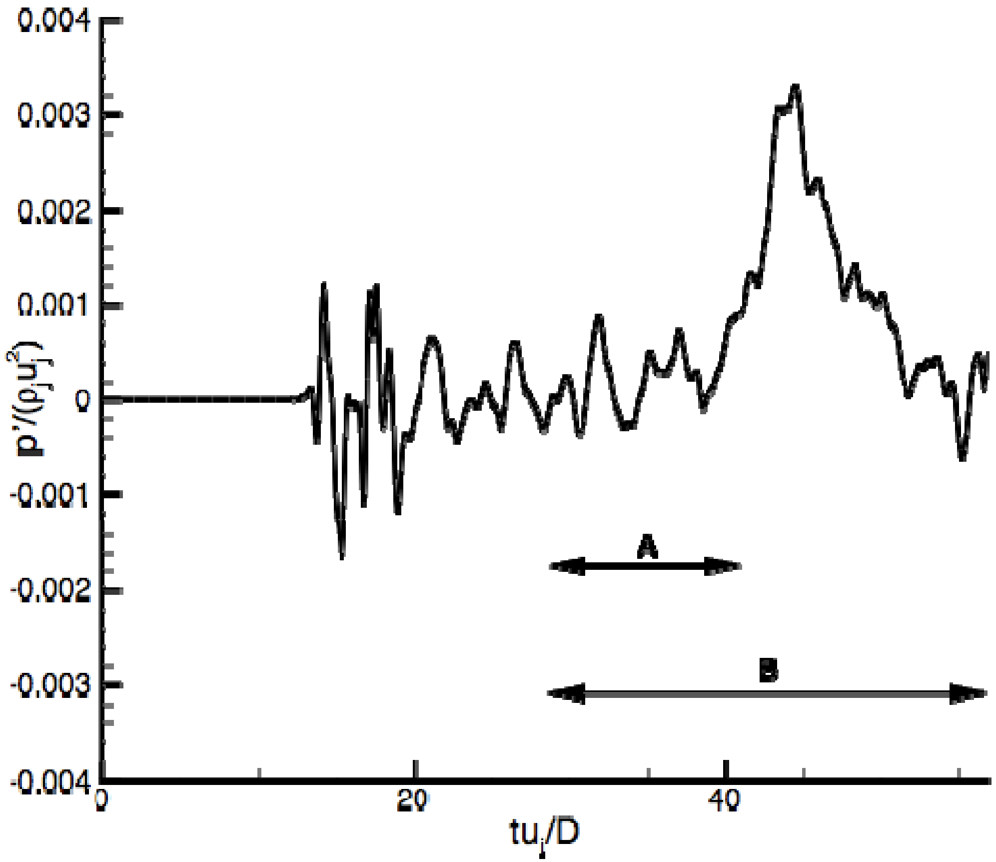

SJ (s<1): Side-Jet Phenomenon

- Hallberg et al. (Phys. Fluids, 2007)
- Depends on initial shear layer momentum thickness
- LES has larger initial shear layer thickness and should experience a stronger side jet phenomenon

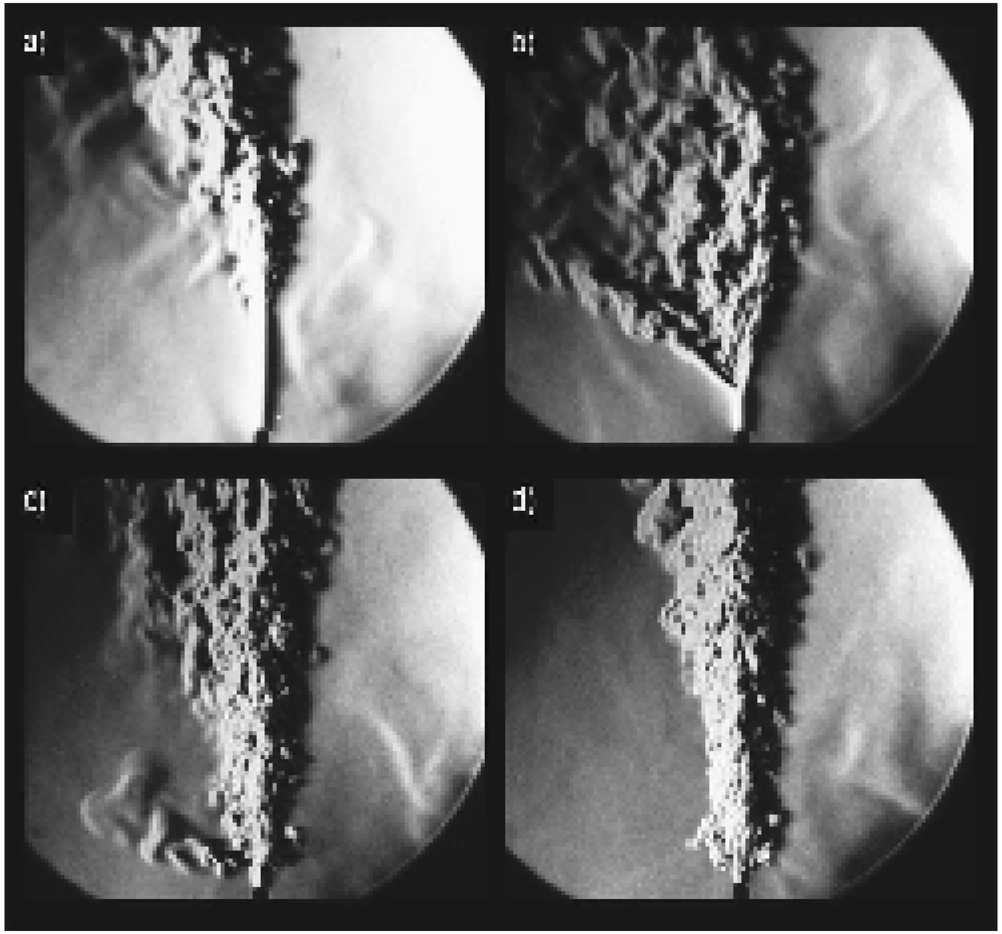

FIG. 2. Schlieren images of helium jets in the absence of coflow as a function of initial shear layer momentum thickness. (a) D/θ_o=24.1, (b) 26.3, (c) 33.8, and (d) 42.7.

SJ (s<1): s = 0.14 LES

SJ (s<1) DNS – LES Comparison

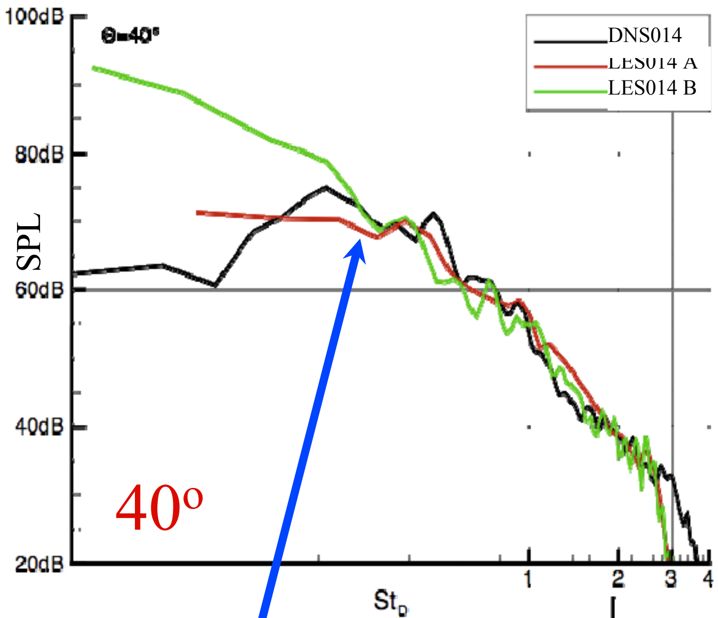

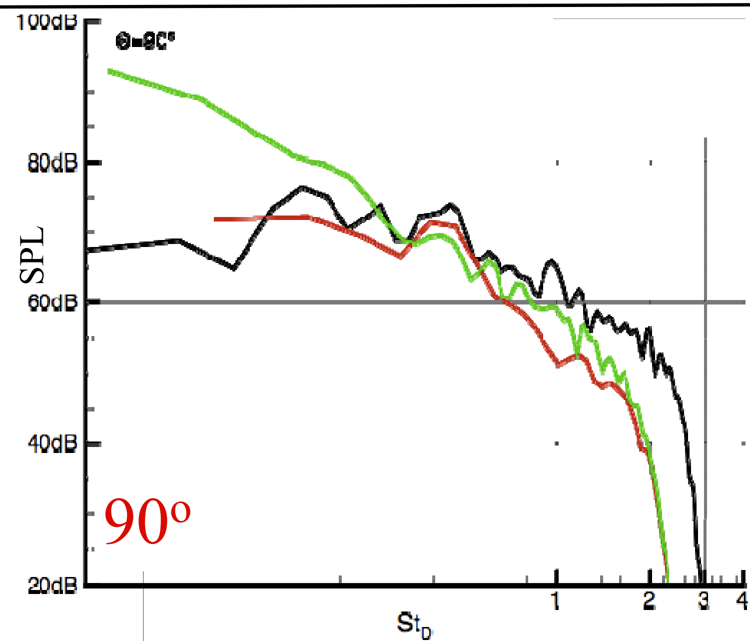

Additional simulation with shorter time series, excluding the burst phenomenon, closer to the PSD signal of the DNS

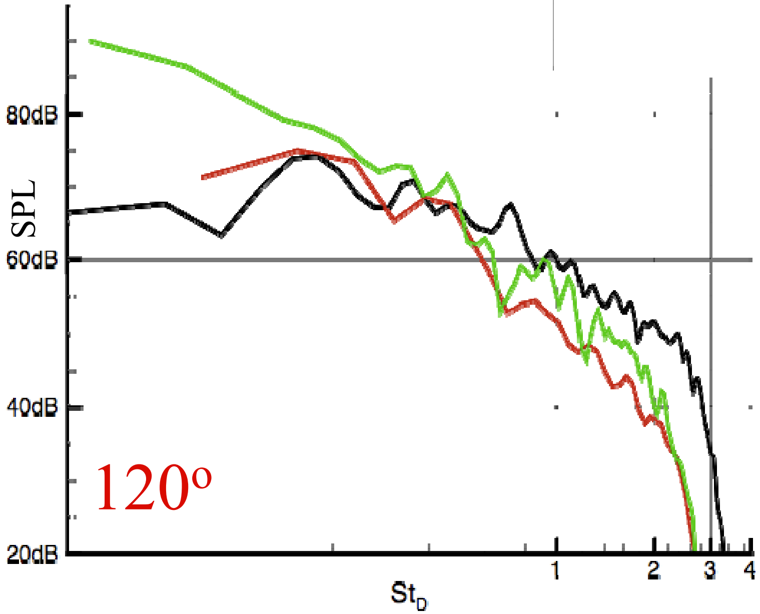

Coming Up

Introduction

Numerical Method

- flow field
- acoustic field

Results (Fluid Mechanics, Acoustics)

- single jet

$\rightarrow$ s (density ratio jet/freestream) = 1

$\rightarrow$ s > 1

$\rightarrow$ s < 1

- coaxial jet

Conclusions

Coaxial Jet Configuration (CJC)

Coaxial Jet with Short Cowl Nozzle (SCN), CoJeN specifications

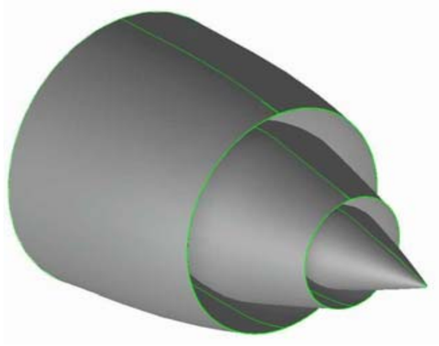

Schematic of short-cowl nozzle

© qinetiq

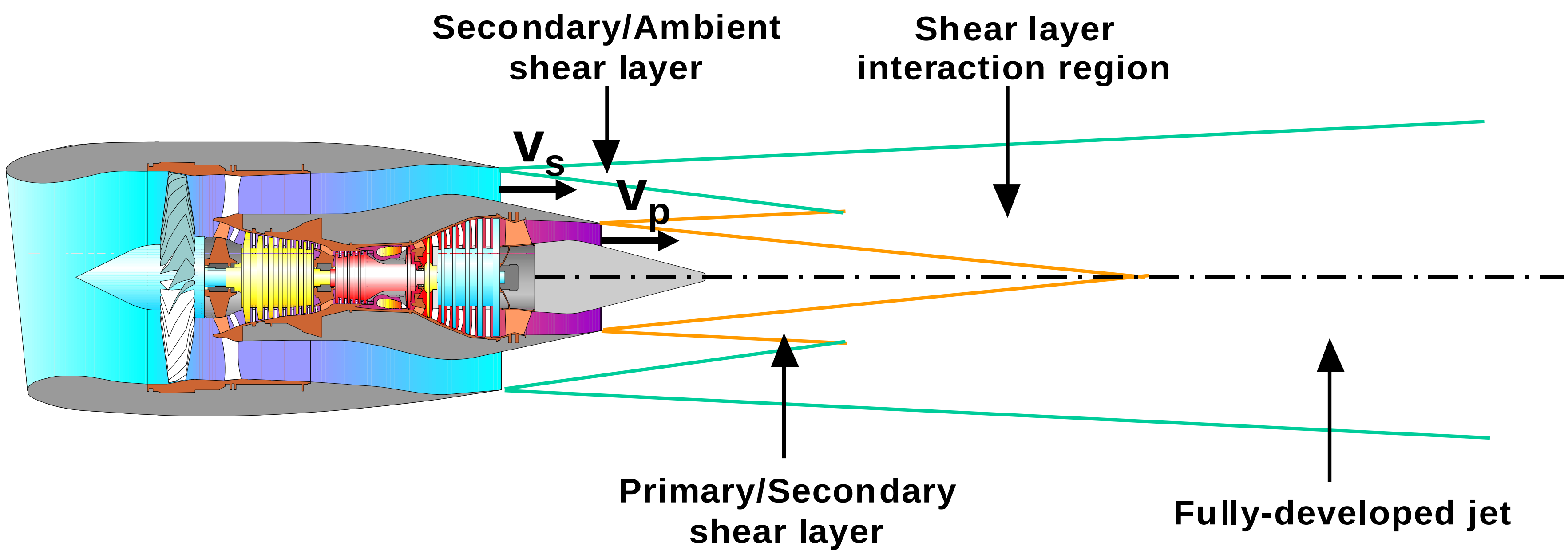

CJC: Jet Configuration

	U_p/U_s	T_p/T_s	T_s/T_a	U_p/a_p	U_s/a_s
cj_c	1.1	1.0	1.0	1.0	0.9
cj_{h1}	1.1	2.7	1.0	0.6	0.9
cj_{h2}	1.6	2.7	1.0	0.88	0.9

- **Coplanar jets without nozzle, $Re_D = 4.0\text{x}10^5$**
- **Artificial forcing (Bogey & Bailly, AIAA J., 43, 2005)**

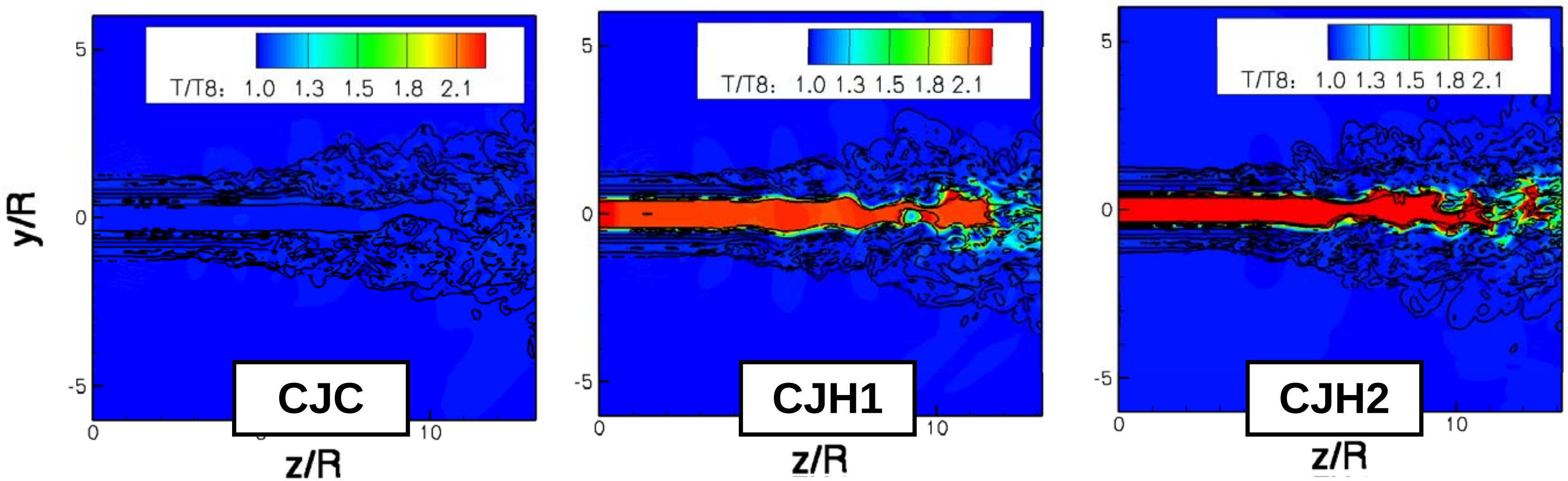

CJC: Grid Topology & Computational Setup

RWTH Aachen

mean inflow profile from RANS simulation

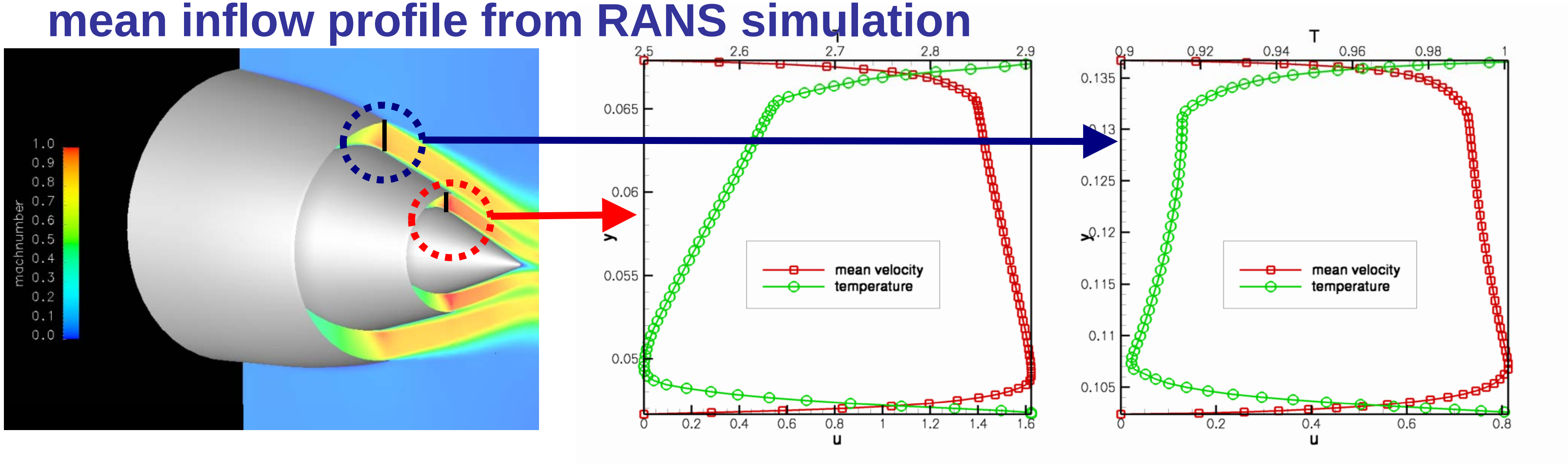

bowl shaped LES grid: $22x10^6$ cells

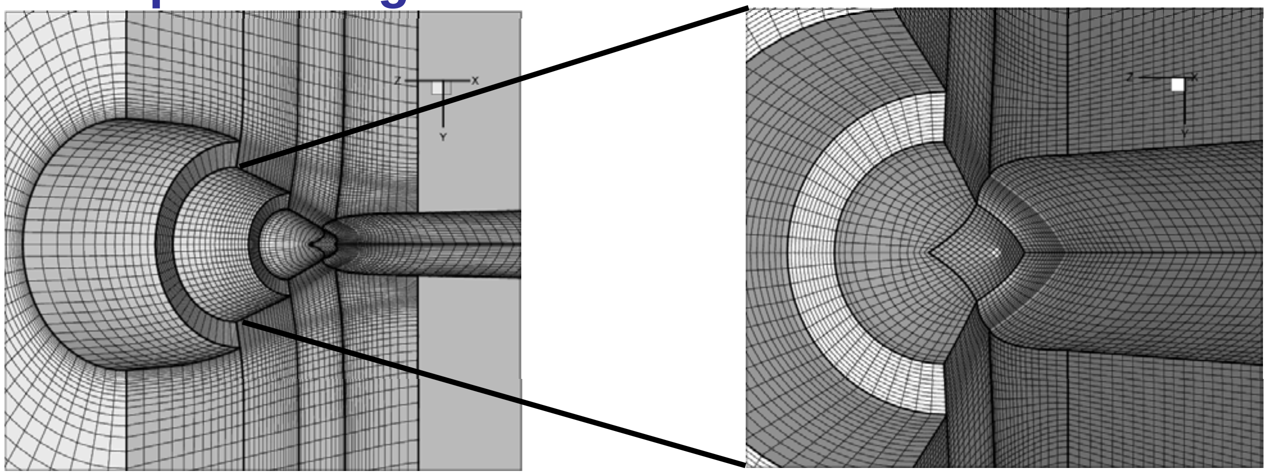

CJC: Vortical Structures

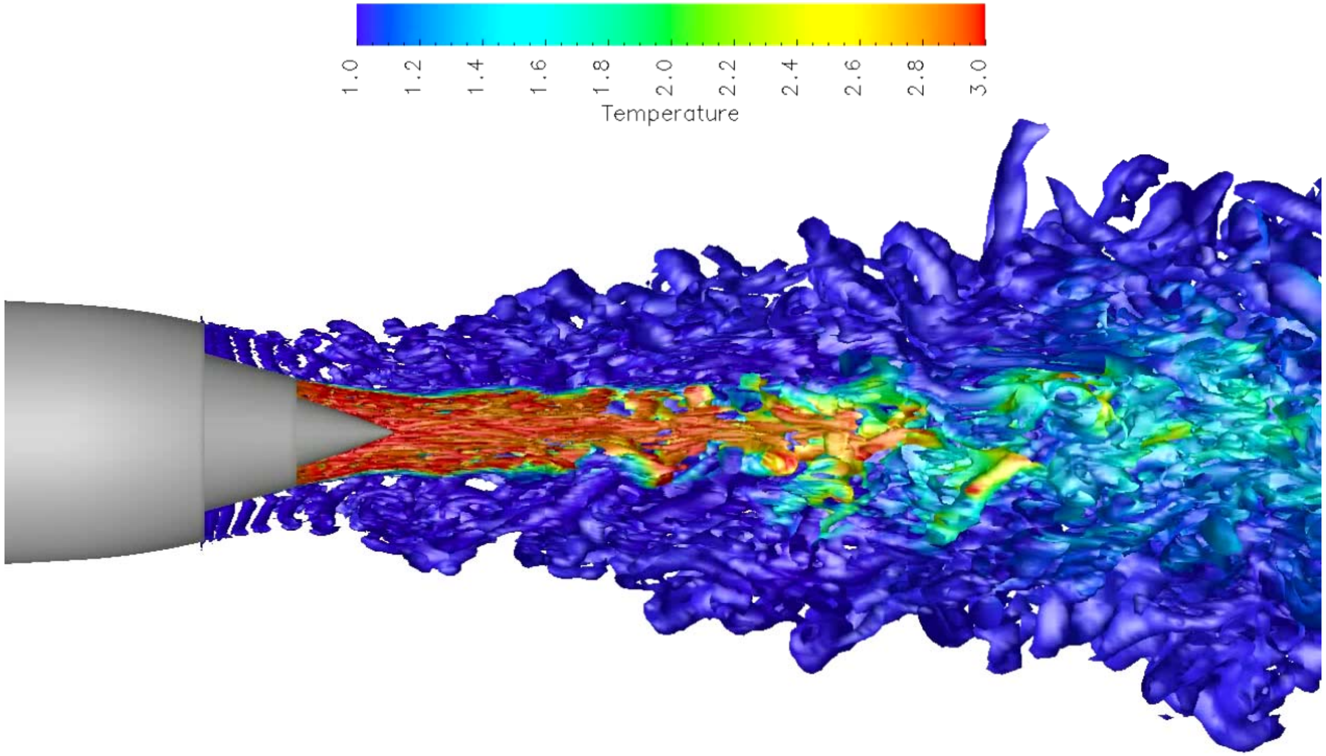

λ_2 contours
colored with temperature

CJC: Comparison of LES and Experimental Data

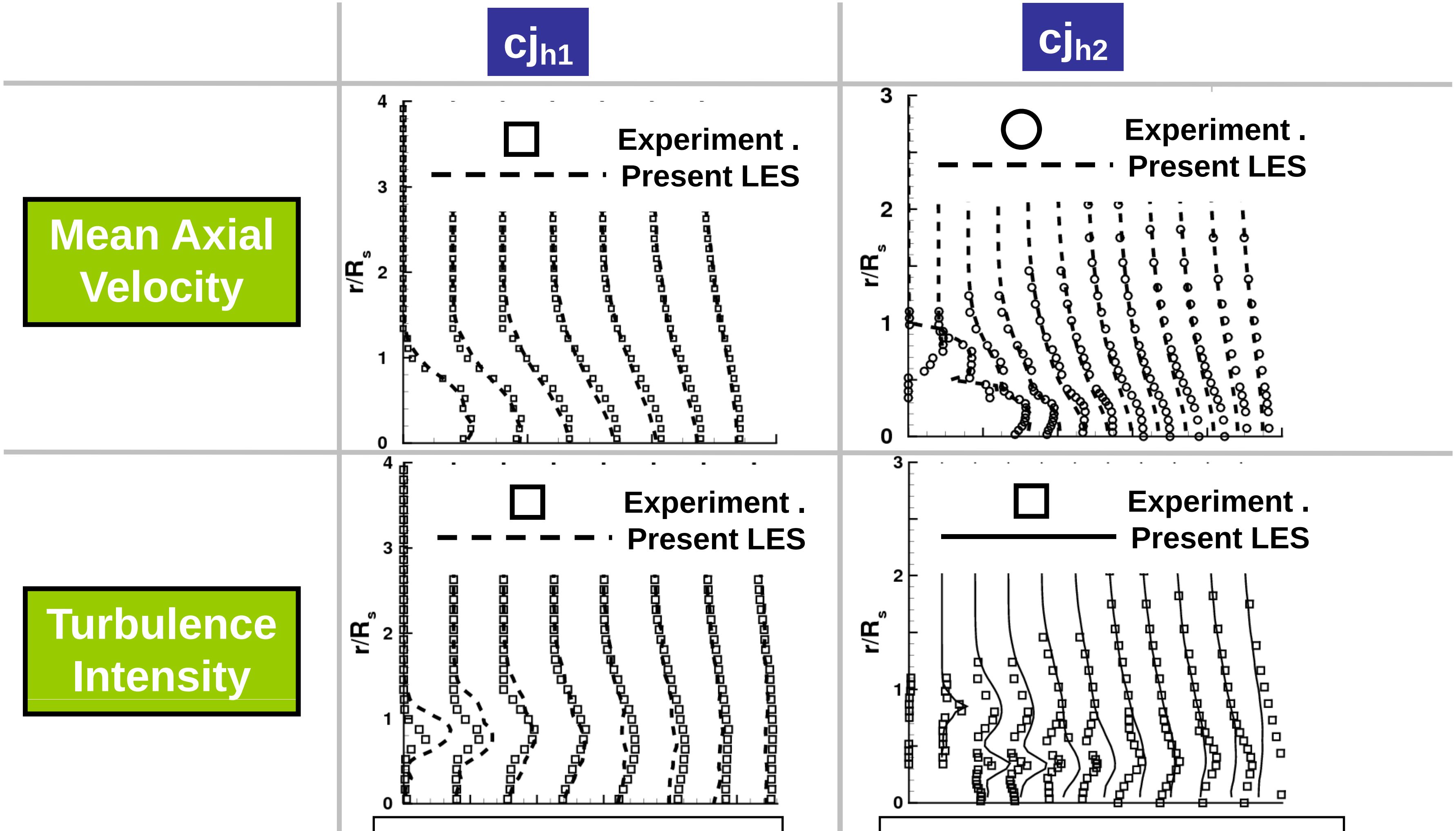

Good agreement with experimental results.

Faster flow development Acceptable agreement

CJC: Instantaneous Contours of Flow and Acoustic Fields

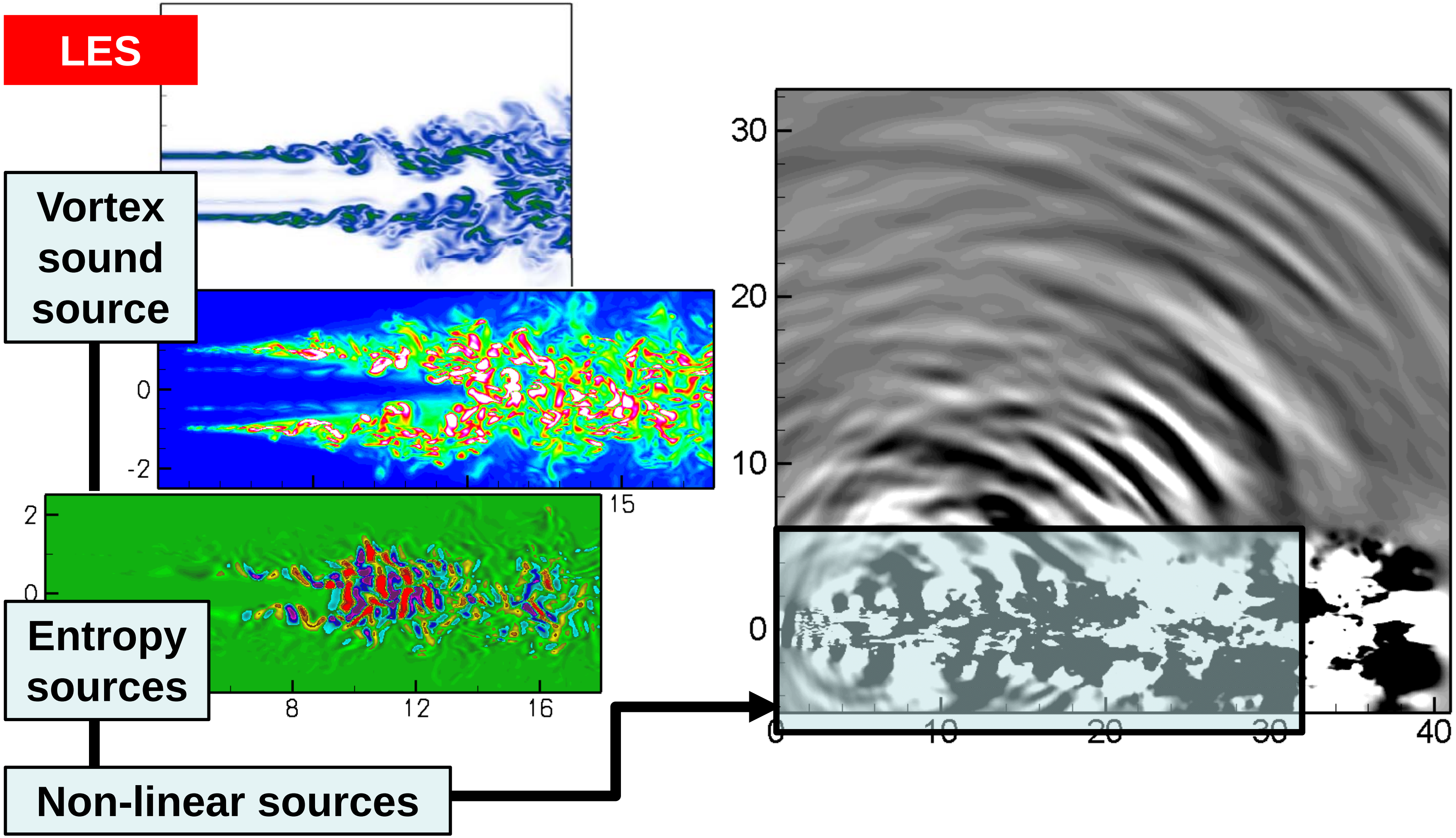

CJC: OASPL
Cold (cjc) and Hot (cjh1) CJ

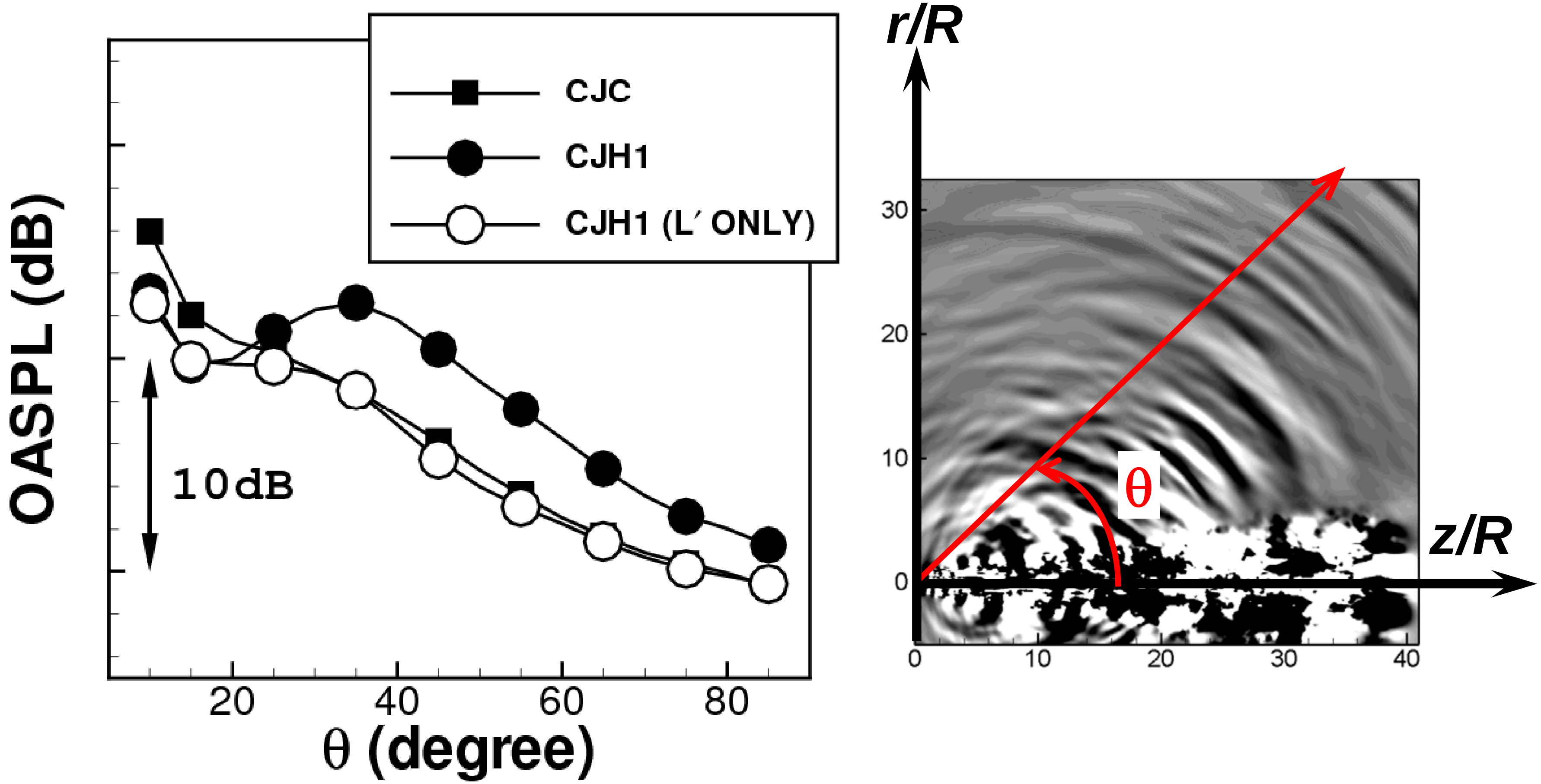

CJC: Heat Impact on Vortex Sound Source (L’)

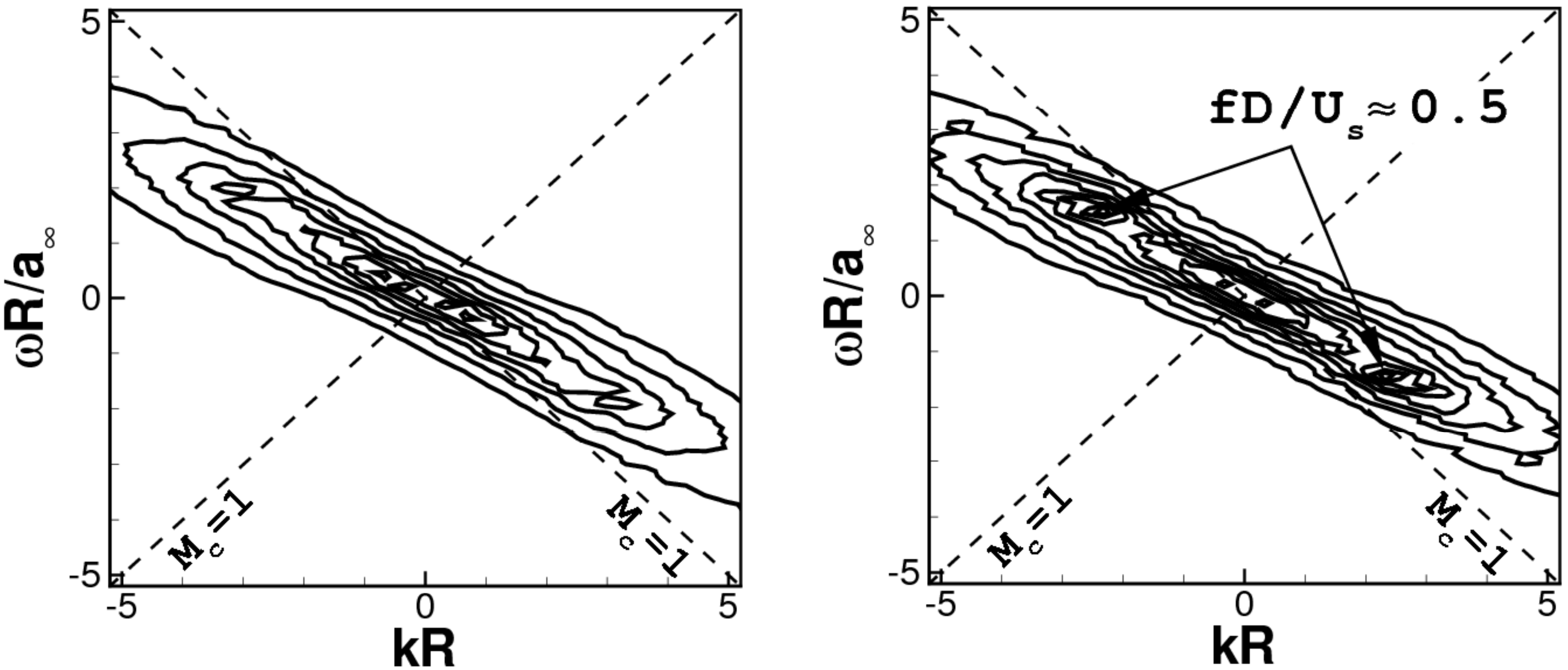

- Additional spectral peaks at fD/U_s=0.5 of the hot coaxial jet : the corresponding phase velocity $M_c < 1$ (poor acoustic efficiency)
- Beyond the sonic speed $M_c > 1$ (no significant difference)
- Vortex sound source (L′) is hardly impacted by the heated jet.

CJC: OASPL
cjh1, cjh2, and Exp. Data

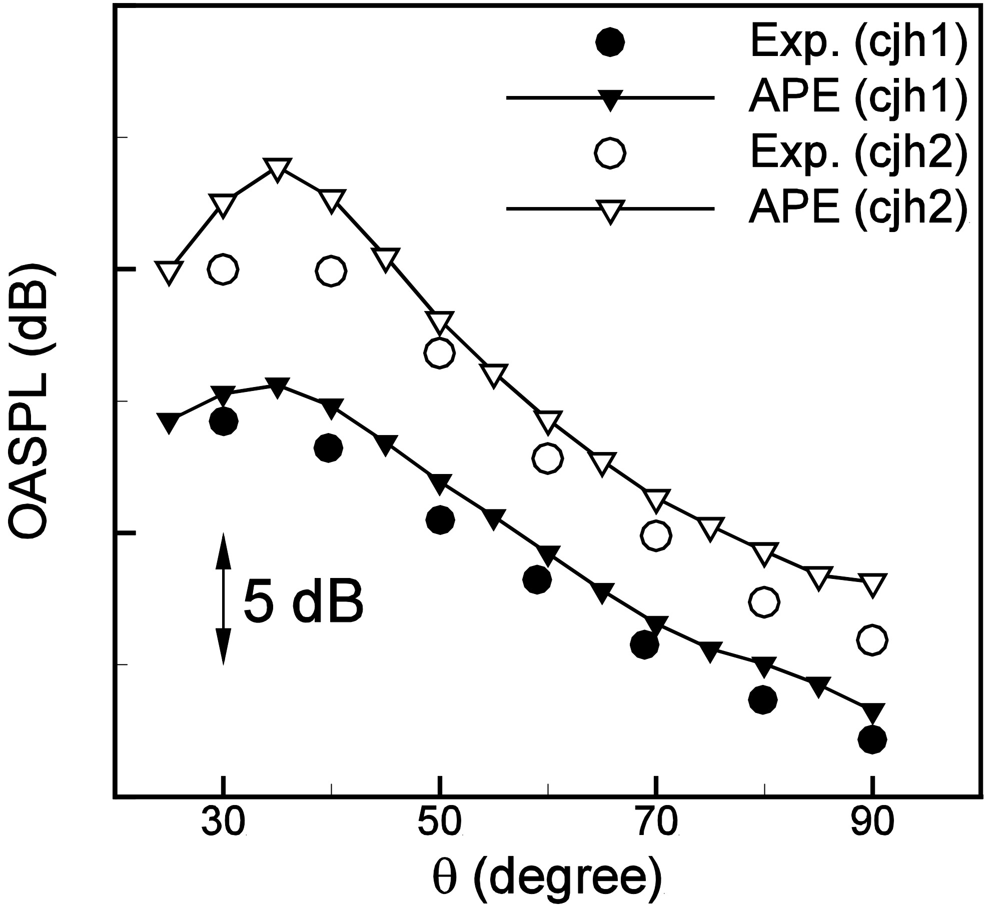

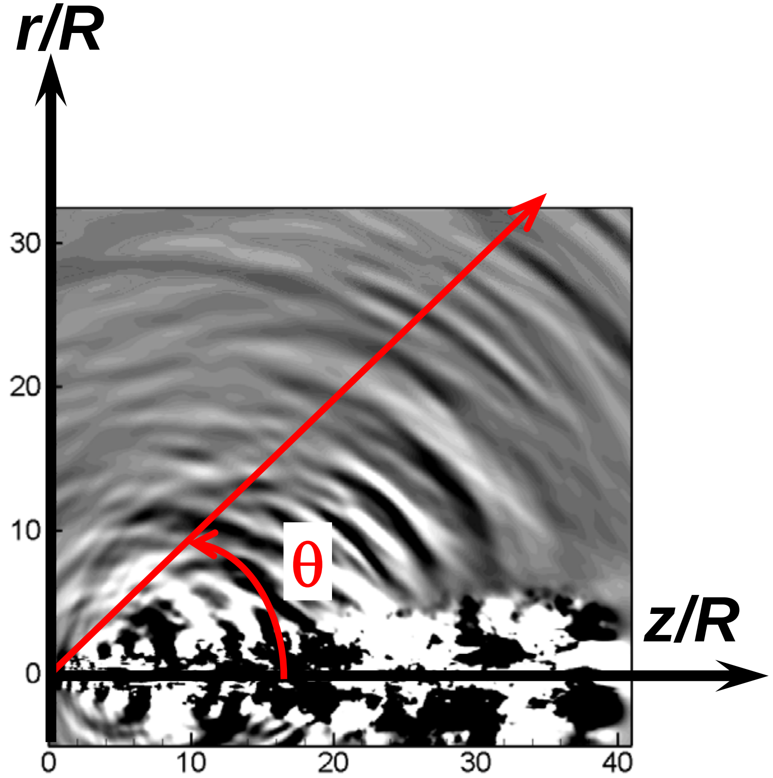

• **Convincing agreement of the LES results and the experimental data**

CJC: Sound Spectra at r_p=40R

Downstream Acoustics

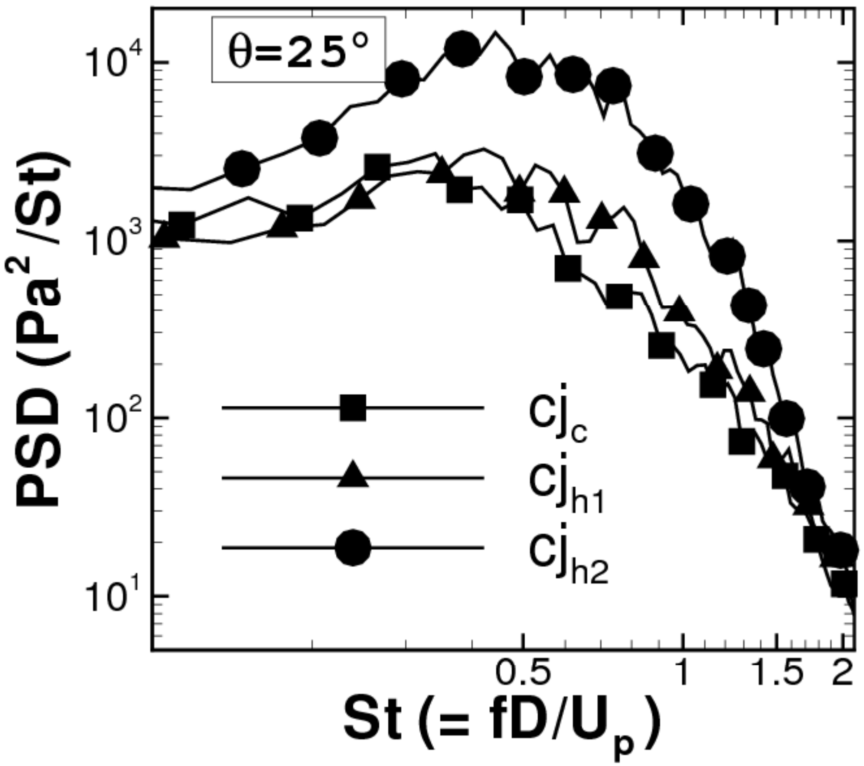

Sideline Acoustics

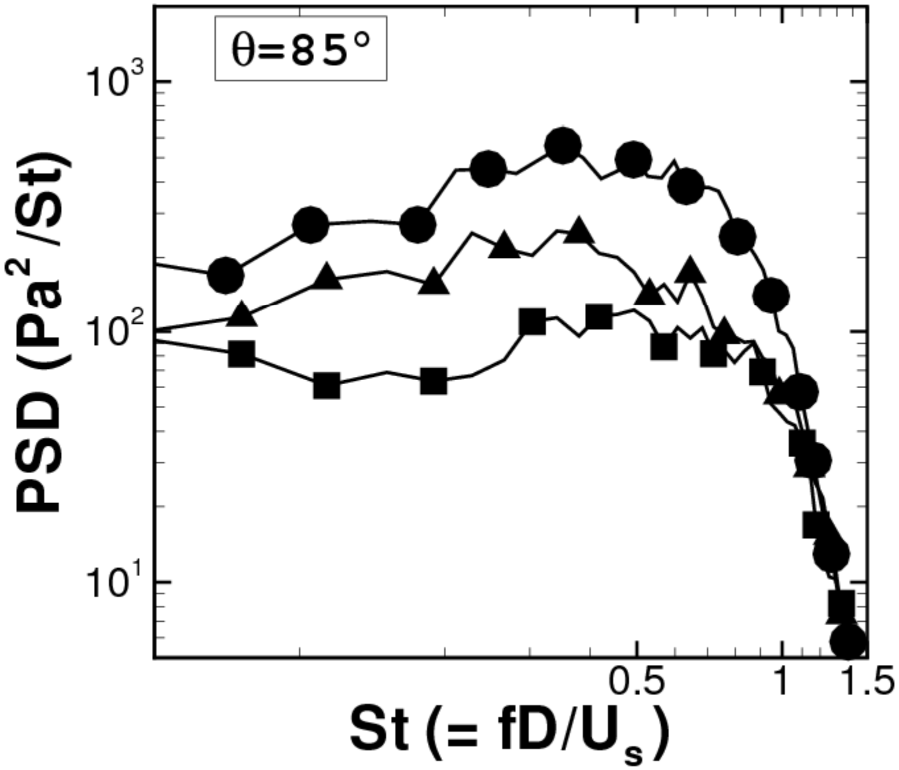

CJC: Entropy Sources in Hot Coaxial Jets

RWTH Aachen

$$\mathbf{Q}_{e,m} = T'\nabla\overline{s} - s'\nabla\overline{T}$$

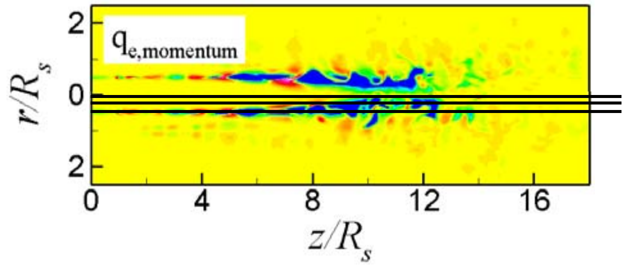

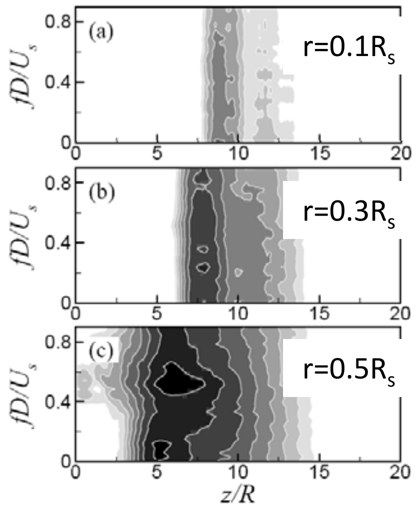

Source spectra

$$\mathbf{Q}_{e,c} = \frac{\overline{\rho}}{c_p}\frac{\overline{D}s'}{Dt}$$

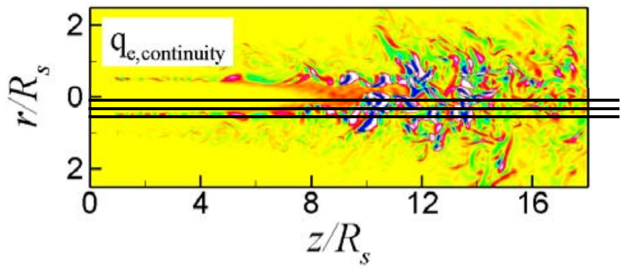

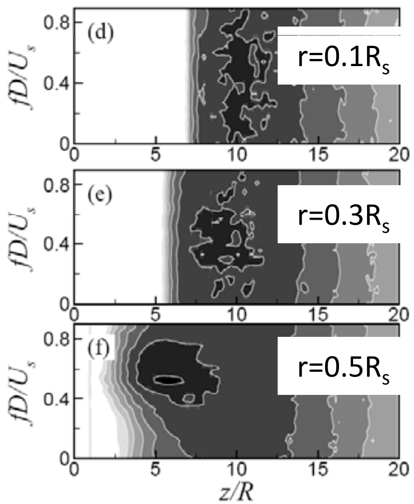

CJC: Entropy Sources in Hot Coaxial Jets

$$Q_{e,m} = T'\nabla\overline{s} - s'\nabla\overline{T}$$

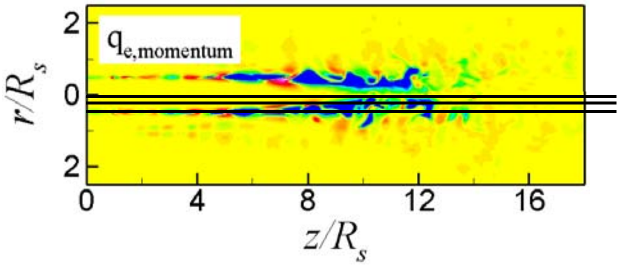

$$Q_{e,c} = \frac{\overline{\rho}}{c_p}\frac{\overline{D}s'}{Dt}$$

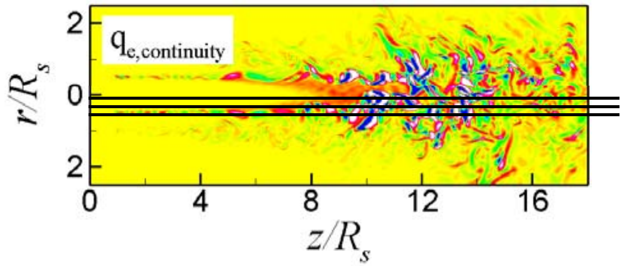

Source spectra

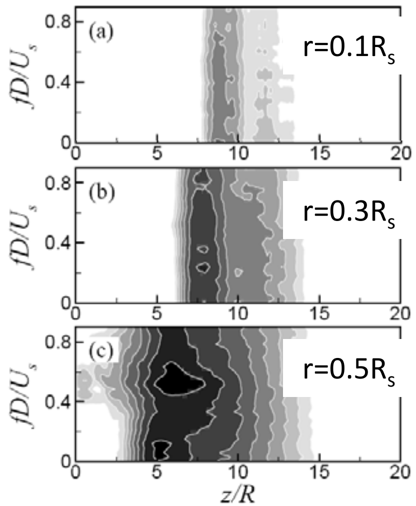

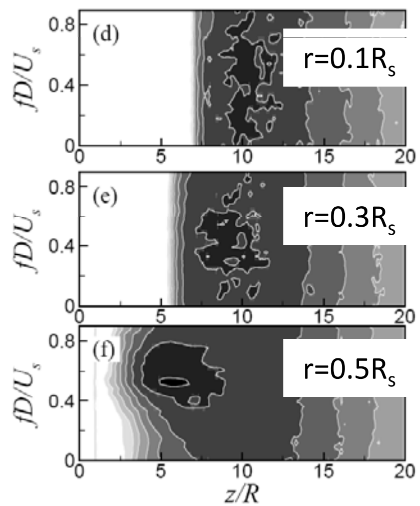

$(Q_{e,m})_{r.m.s.}$

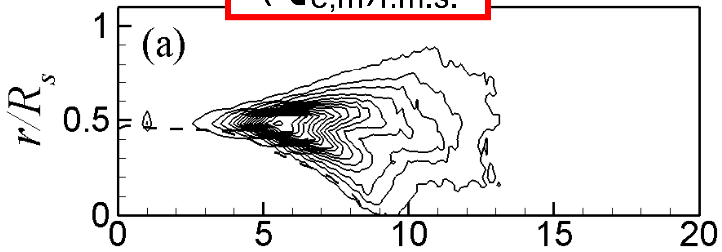

$(Q_{e.c})_{r.m.s.}$

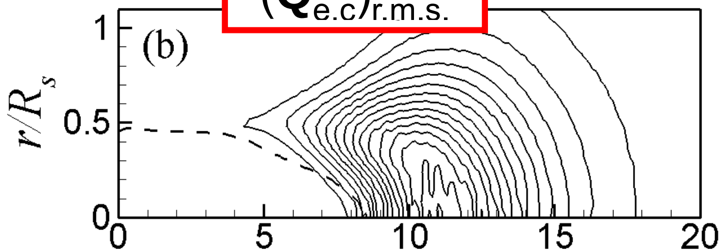

CJC: Entropy Sources in Hot Coaxial Jets

$$\mathbf{Q}_{e,m} = T'\nabla\bar{s} - s'\nabla\bar{T}$$

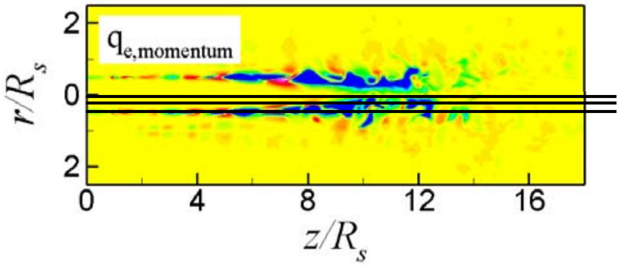

$$\mathbf{Q}_{e,c} = \frac{\bar{\rho}}{c_p}\frac{\overline{D}s'}{Dt}$$

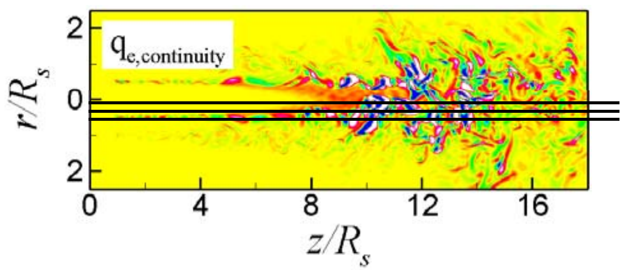

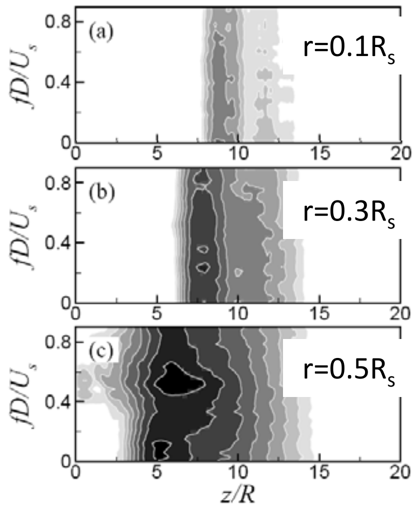

Source spectra

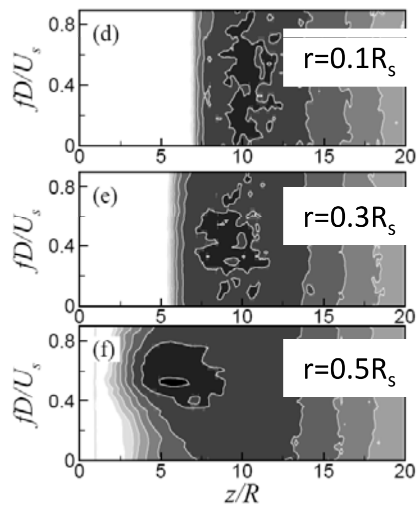

$(\mathbf{Q}_{e,m})_{r.m.s.}$

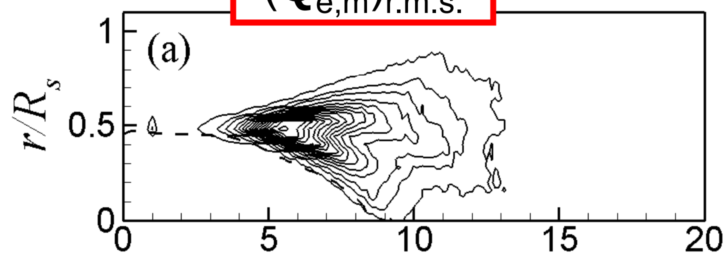

Spectral Peaks

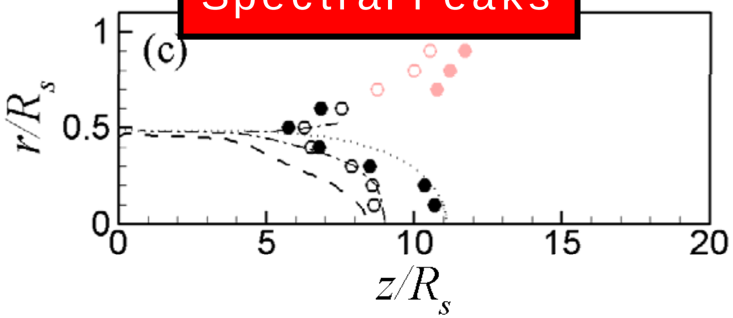

$(\mathbf{Q}_{e.c})_{r.m.s.}$

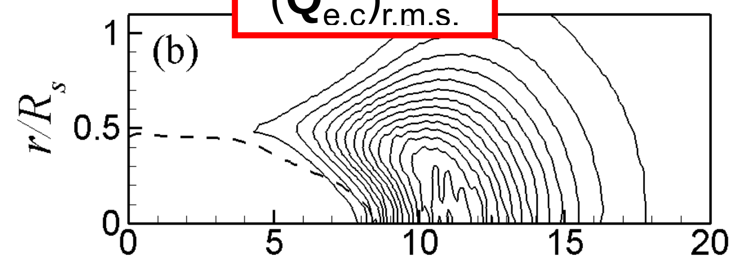

CJC: OASPL cj_{h2}
Lamb vs. Full Source

Directivity at $r=60R_s$

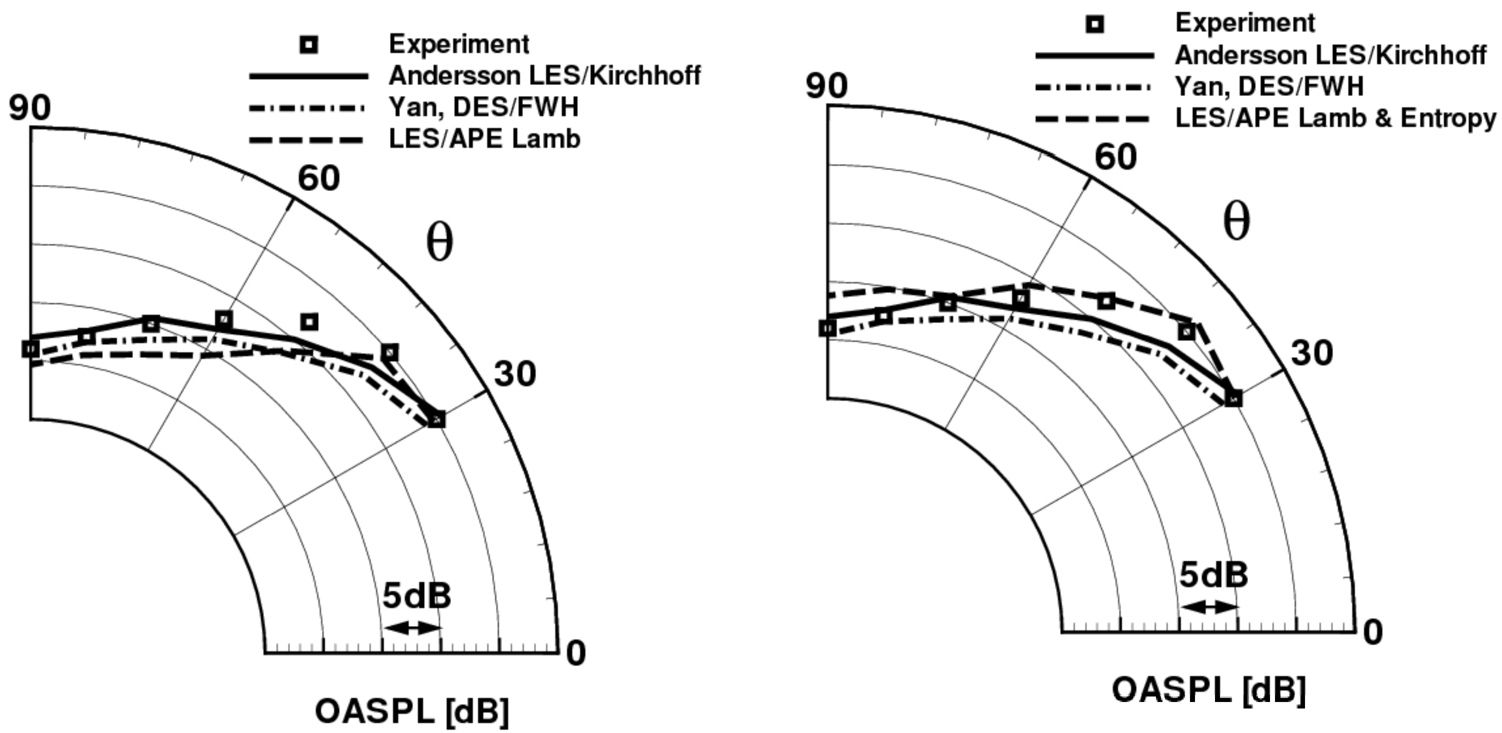

- *Lamb vector captures noise for angles up to 40 degree to jet axis*
- *Entropy related sources important for obtuse angles*

Coming Up

Introduction

Numerical Method

- flow field
- acoustic field

Results (Fluid Mechanics, Acoustics)

- single jet
  - $\rightarrow$ s (density ratio jet/freestream) = 1
  - $\rightarrow$ s > 1
  - $\rightarrow$ s < 1
- coaxial jet

Conclusions

Conclusions I

RWTH Aachen

Numerical Method:

- hybrid CFD/CAA approach yields high-quality results

Single Jet (s > 1):

- comparison of CO_2 and cooled-air jets
- OASPL possesses a max. difference of 3 dB
- OASPL (CO_2) > OASPL (cooled-air jet) at $0° \leq \theta \leq 30°$
- PSD (cooled-air jet) > PSD (CO_2) at $St_D \geq 0.5$ and $\theta \geq 35°$;
  PSD (cooled-air jet) < PSD (CO_2) at $St_D \leq 0.2$

Single Jet (s < 1):

- an absolute instability exists at s = 0.14
- absolute instability dominates sound emission
- size of filter width reduces TKE content and results in an approx. 3 dB difference between filtered and non-filtered data
- LES yields high-quality results at $St_D \leq 1.5$
- side jet determines the low-frequency SPL distribution

Conclusions II

Single Jet ($s \neq 1$):

- **$s < 1$ jet undergoes a much more sudden breakdown than the $s > 1$ jet**
- **the smaller s, the more upstream the onset of the centerline velocity decay**

Coaxial Jet:

- **vortex sound source is hardly impacted by the temperature gradient**
- **entropy sources determine the qualitative and quantitative directivity and OASPL**
- **especially the OASPL at $30° \leq \theta \leq 60°$ is determined by the entropy sources**

High Reynolds # DNS, s=1.52

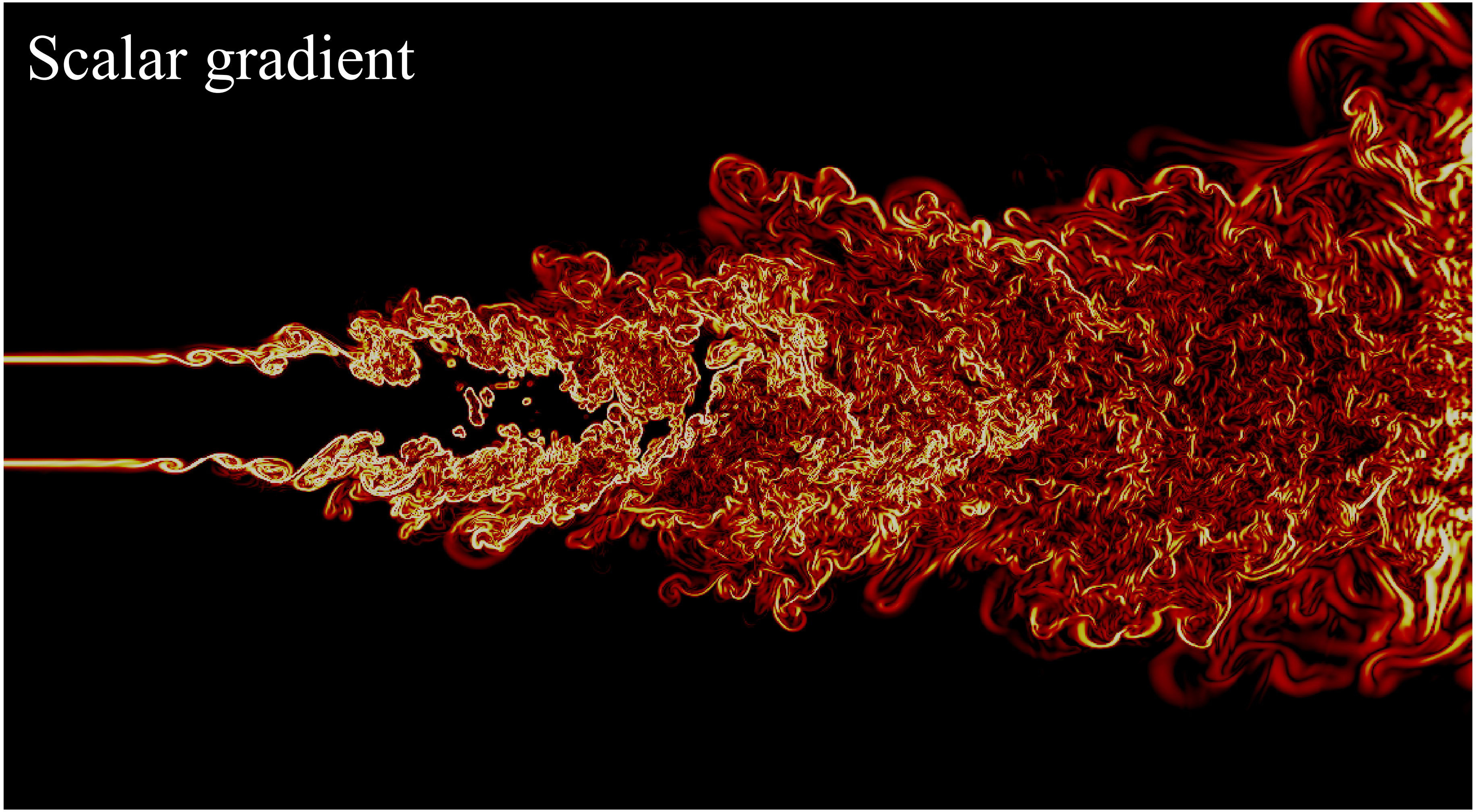

High Reynolds # DNS, s=1.52

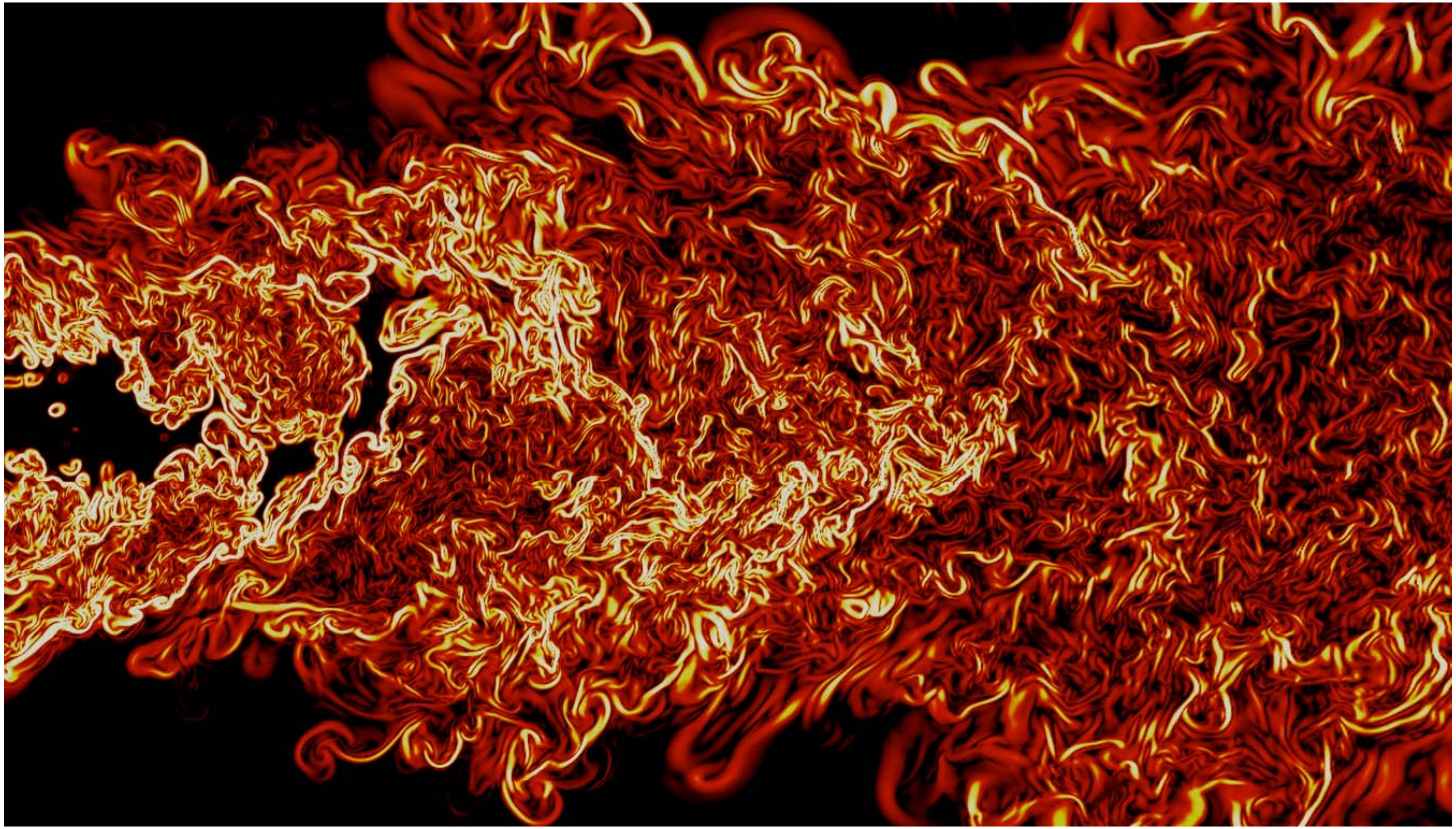

High Reynolds # DNS, s = 1

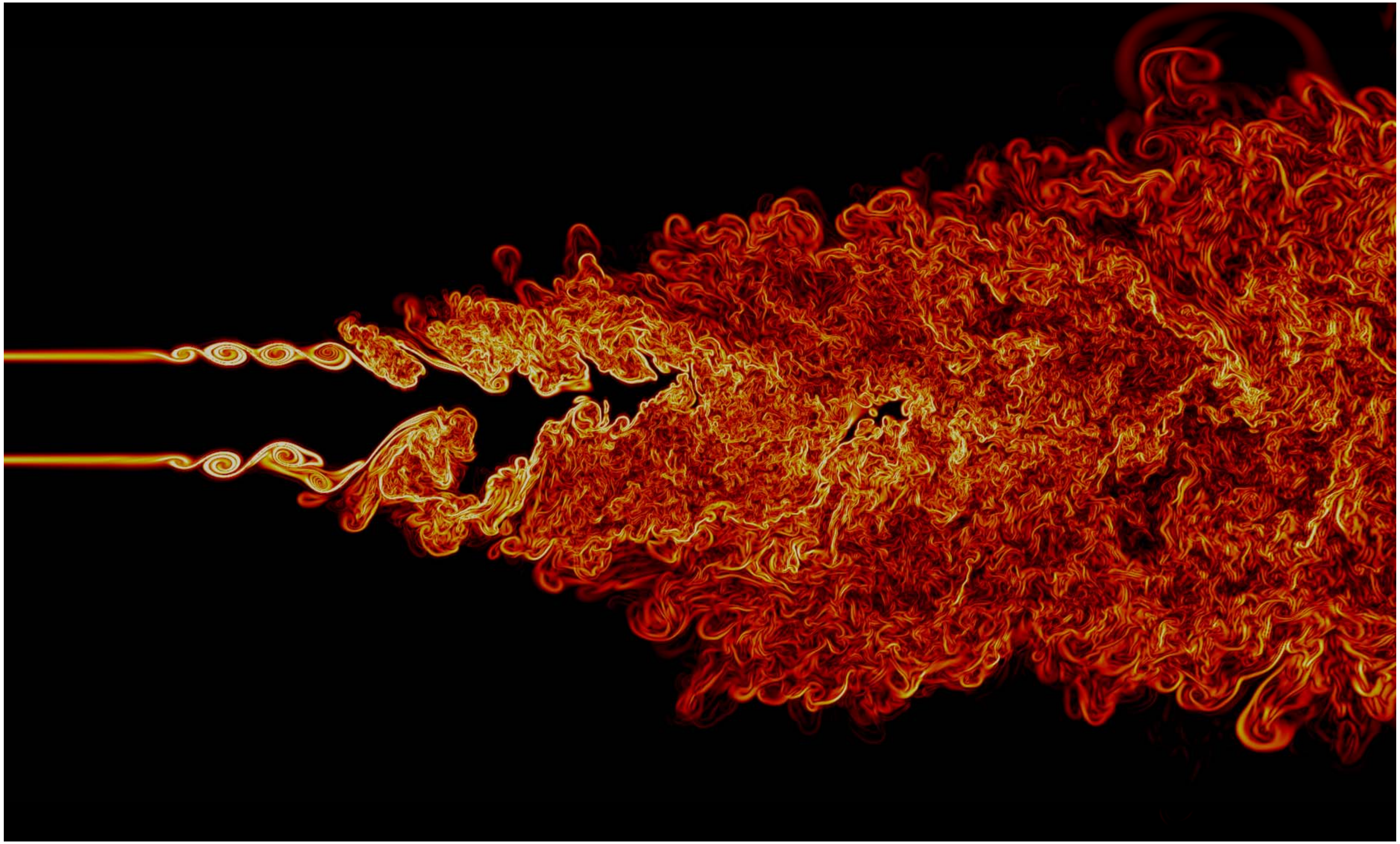

High Reynolds # DNS, s = 1

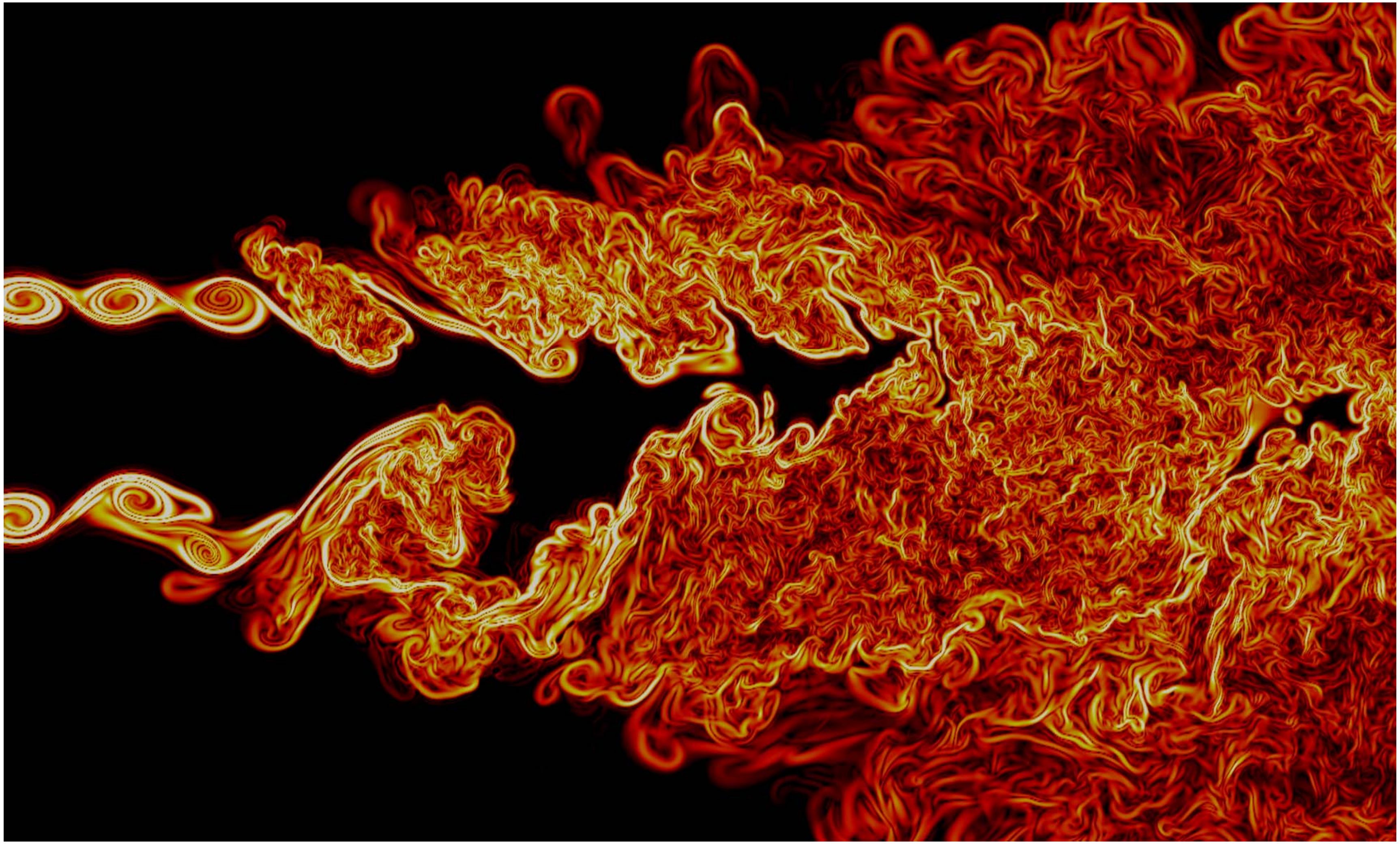

High Reynolds # DNS, s = 1

RWTH Aachen

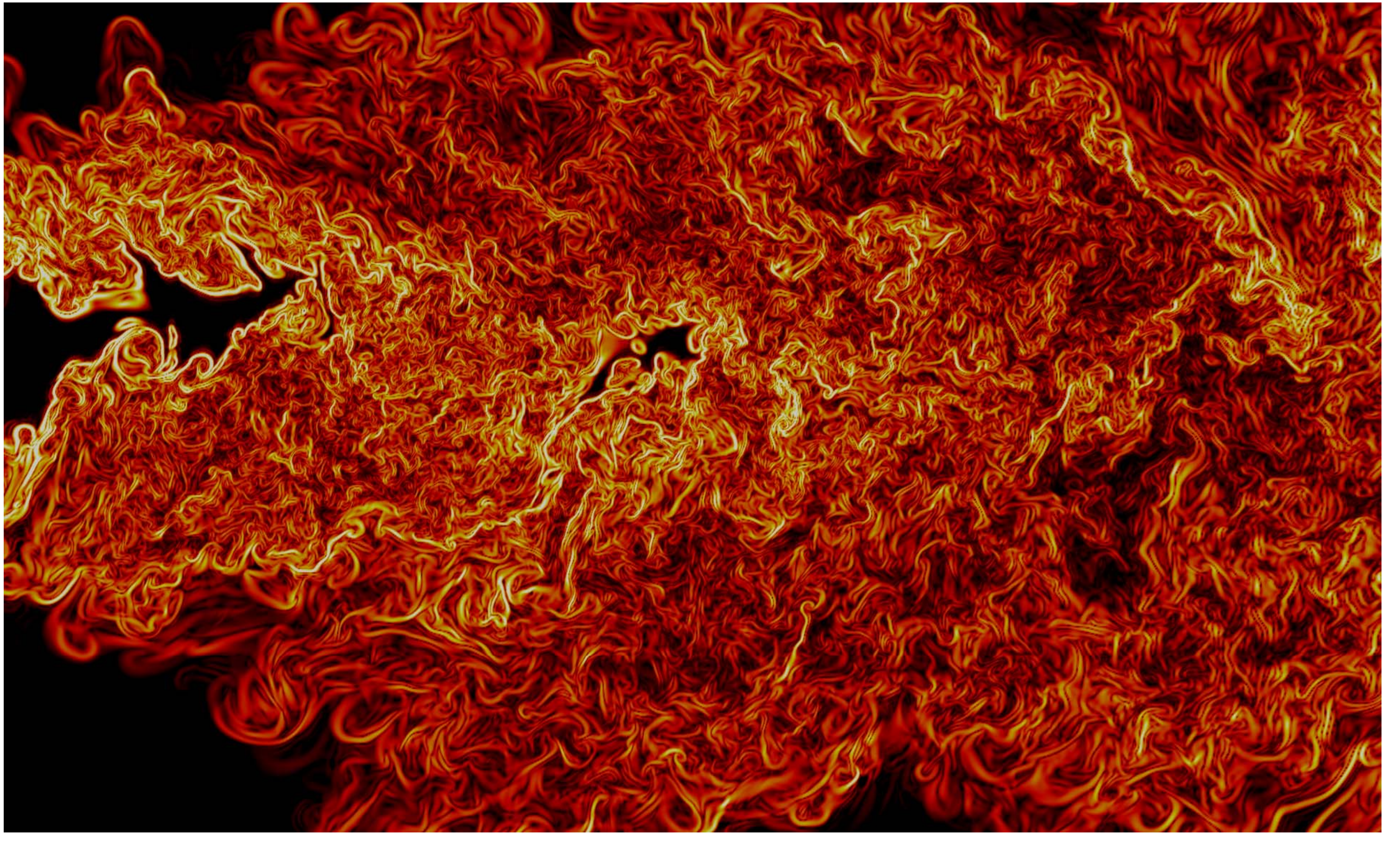

RMS Distribution

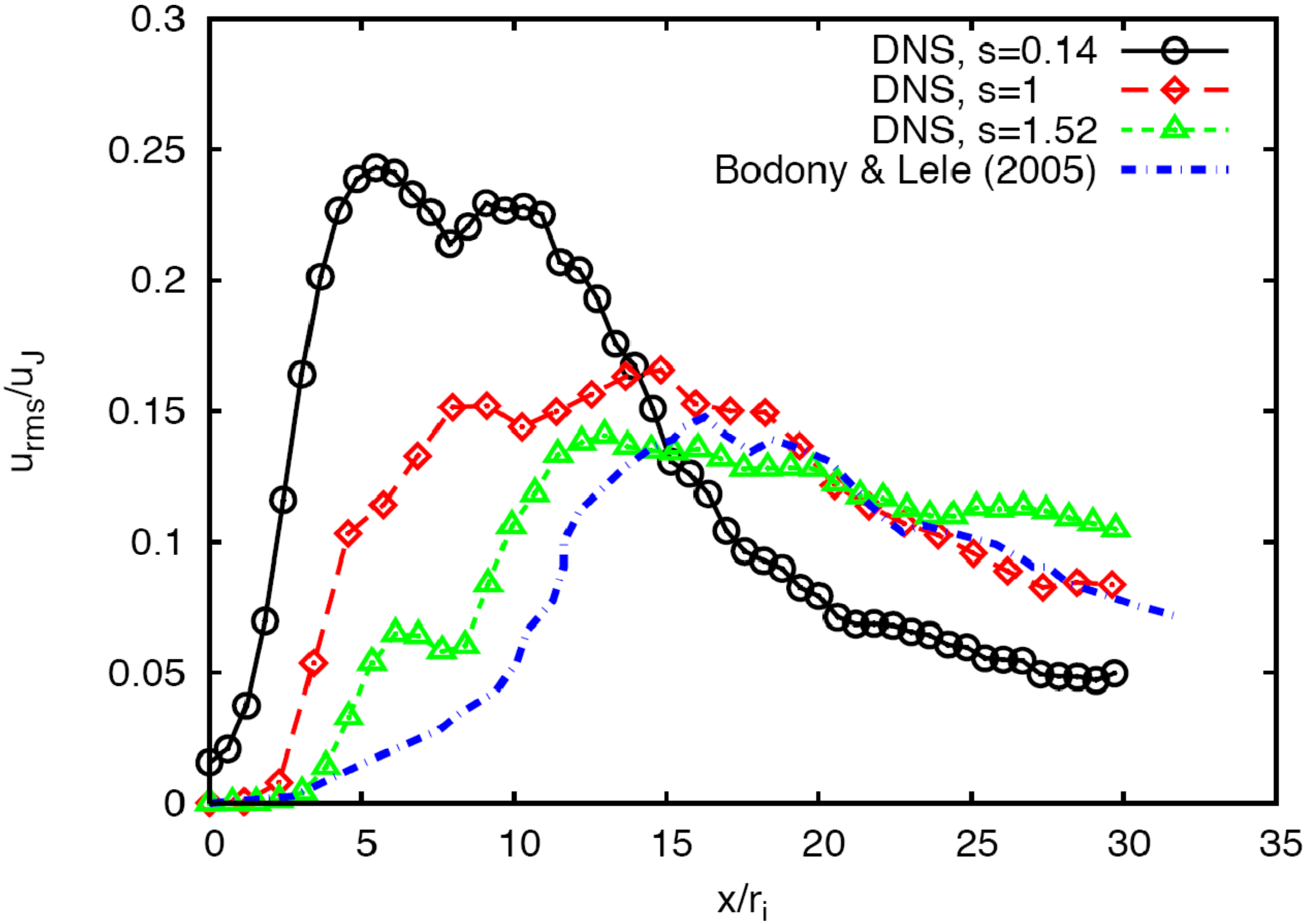

RMS Distribution

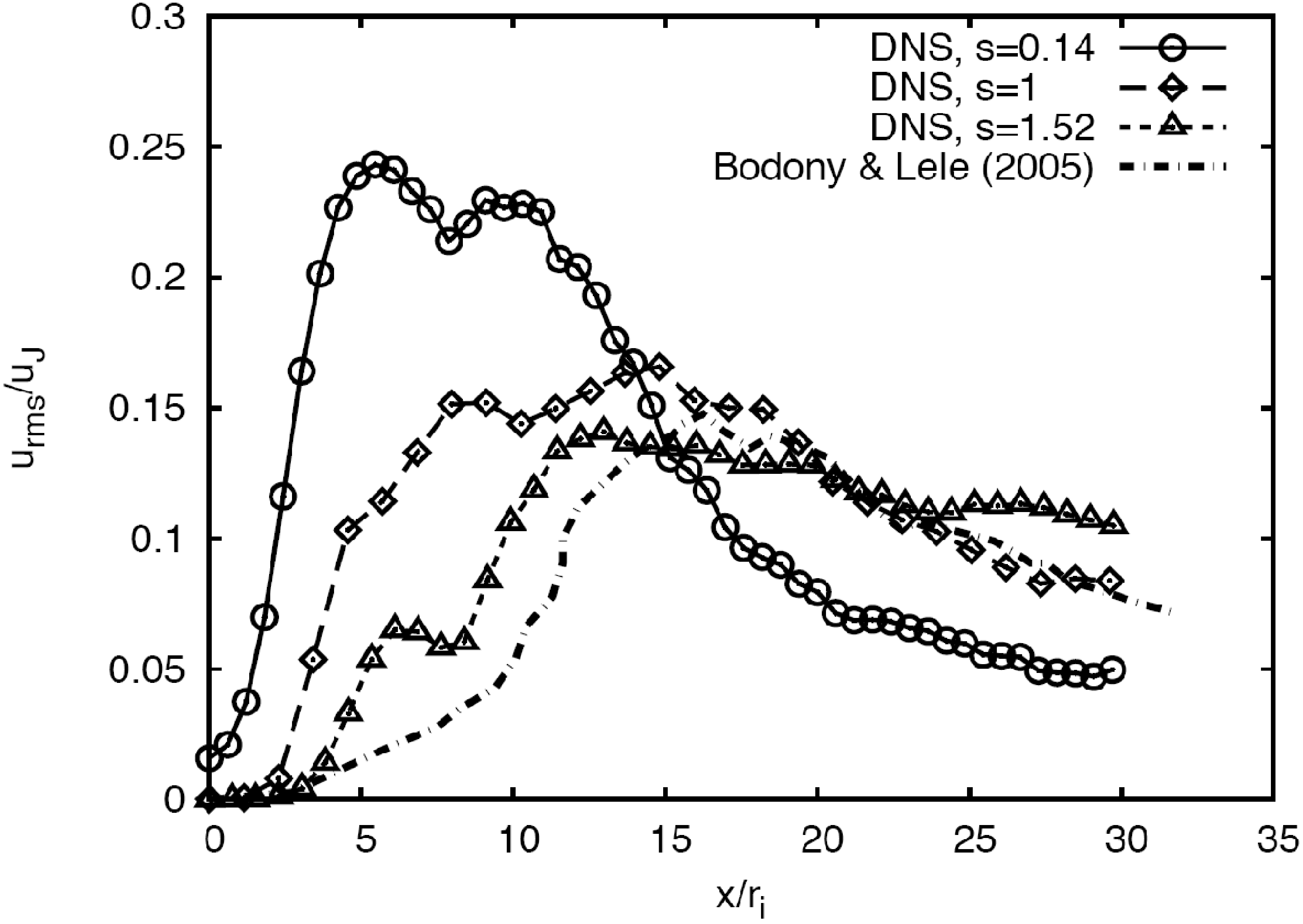

References

Ewert, R. and Schröder, W., "Acoustic perturbation equations based on flow decomposition via source filtering", *Journal of Computational Physics*, Vol. 188, pp. 365-398, 2003.

Ewert, R. and Schröder, W., "On the Simulation of Trailing Edge Noise with a Hybrid LES/APE Method", *Journal of Sound and Vibration*, Vol. 270, pp. 509-524, 2004.

Schröder, W. and Ewert, R., "LES-CAA Coupling", *LES for Acoustics*, Cambridge University Press, 2005.

Gröschel, E. R., Meinke, M., and Schröder, W., "Noise prediction for a turbulent jet using an LES/CAA method", *AIAA Paper 2005-3039*, 2005

Gröschel, E.R., Schröder, W., and M. Meinke, "Noise generation mechanisms in single and coaxial jets", *AIAA Paper 2006-2592,* 2006.

Gröschel, E., Schröder, W., Renze, P., Meinke, M., and Comte, P., "Noise prediction for a turbulent jet using different hybrid methods", *Computers and Fluids*, 37(4), pp. 414-426, 2008.

Gröschel, E., Renze, P., Schröder, W., and Meinke, M., "Towards noise reduction of coaxial jets", *AIAA Paper 2007-3646*, 2007.

Koh, S.R., Gröschel, E., Meinke, M., and Schröder, W., "Numerical analysis of sound sources in high Reynolds number single jets", *AIAA Paper 2007-3591*, 2007.

Koh, S.R., Schröder, W., and Meinke, M., "Turbulence and Heat Excited Noise Sources in Single and Coaxial Jets", *Journal of Sound and Vibration*, Vol. 329, pp. 786 – 803, 2010.

Schröder, W., "Hybrid Simulation of Flow Induced Noise", *Nordrhein-Westfälische Akademie der Wissenschaften*, Vorträge I 27, Schöningh, 2009.

Koh, S.R., Schröder, W., and Gröschel, E., Meinke, M., and Comte, P., "Noise Prediction for Turbulent Coaxial Jets", *Notes on Numerical Fluid Mechanics and Multidisciplinary Design*, Vol. 104, pp. 99-120, 2009.

Koh, S.R., Schröder, W., and Meinke, M., "Sound generation control by fluid bleeding", *AIAA Paper 2009-3225*, 2009.

Schlegel, M., Noack, B., Lehmann, O., Dillmann, A., Gröschel, E., Schröder, W., Wei, M., Freund, J. B., and Jordan, P. "On Least-Order Flow Representations for Aerodynamics and Aeroacoustics", submitted to *J. Fluid Mech*., August 2009.

Geiser, G., Koh, S.R., Foysi, H., and Schröder, W., "Sound generation of variable density jets", *AIAA Paper 2010-3844,* 2010.

Foysi, H., Geiser, G., Koh, S.R., and Schröder W., "Effect of filter width on sound of variable density jets", *AIAA Paper 2010-3845,* 2010.

Koh, S.R., Schröder, W., and Meinke, M., "Numerical study of noise reduction via wall turbulence control", *AIAA Paper 2010-3990,* 2010.